Helene Fonnes

Determining the impact of the R249S mutation on *Tp53* gene on cell survivability during AFB1 exposure

Bachelor Thesis in

Biomedical Laboratory Science

June 2022

NTNU

UCLy
LYON CATHOLIC UNIVERSITY

Preface

This report is written as a final product of the Bachelor project at the Bachelor's degree programme performed at the Department of Biomedical Laboratory Science at the Norwegian University of Science and Technology (NTNU) in Trondheim. The objective is given by associate professor Fanny Odet at the Catholic University of Lyon (UCLy). The Bachelor project was performed in the period March to June 2022 in the Team "pôle 7" Biosciences, Technologies and Ethics, which is part of the Confluence Sciences & Humanities Research Unit (EA1598) at UCLy. This multi-thematic transversal unit of UCly was set up in 2020 to support higher education at the School of Biology and Biotechnologies (ESTBB).

Firstly, I want to thank my professional supervisor Fanny Odet, associate professor at UCLy, for all help, explanations, patience, and guidance in both practical and theoretical work. Both Fanny Odet and Kristin Solum Steinsbekk, associate professor at NTNU, have been the reason this internship has been possible, and for that I am grateful. My appreciation extends to my supervisor at NTNU Camilla Wolowczyk, postdoctoral fellow at NTNU, for help with finalizing this written report.

Secondly, I want to thank ESTBB for allowing me to perform my Bachelor project and welcoming me to their laboratory. My appreciation extends to the people at the laboratory and in the research group that made me feel welcomed and introduced me to their specific projects.

Lastly, I would like to extend a huge thank you to Sihem Shgairi and the other interns. Sihem has included me, encouraged me, and spent time talking to me in spite of our language barrier. Paule-Martine Coussoud Béatrix, Farida Yark, Théo Pini and Mélissa Florance have all contributed greatly to making my internship enjoyable.

June 2022, UCLy France

Abstract

Hepatocellular Carcinoma (HCC) is one of the most frequent and malignant cancers worldwide and is found to be endemic in the same geographically areas as high exposure with Aflatoxin B1 (AFB1). AFB1 is a mycotoxin, naturally occurring as a secondary metabolite produced by microfungi that frequently contaminate foods and feeds.

The complete and exact mechanisms of AFB1 hepatocarcinogenesis have not been fully elucidated, however, one major effect of AFB1 is due to the metabolites created when AFB1 is metabolized in the liver. Indeed, the metabolite AFB1-exo-8,9-epoxide have genotoxic effects, causing DNA adducts that most frequently result in a G>T substitution.

A specific hotspot mutation at the third guanine residue of the codon 249 on the *TP53* gene has been identified. The R249S mutation is found in 60 % of patients with HCC in areas where there is high exposure to aflatoxins.

However, these obvious correlations lack direct functional evidence. We therefore developed the project to explore the cell survivability to an AFB1 exposure in the presence and absence of the R249S mutation, and if a long-term treatment with AFB1 would induce this specific mutation in p53 wild type cell lines.

This project used a panel of liver cell lines consisting of HepG2, Hep3B, Mahlavu and HuH7 which all have different mutation status on the *TP53* gene.

Our preliminary experiments on HepG2 (p53-WT), HuH7 (p53 overexpression) and Mahlavu (p53-R249S mutation) using MTT assay showed that the R249S mutation doesn't confer a selective advantage to cells treated with AFB1 at different concentration.

Meanwhile, results from the long-term treatment assay remains currently inconclusive due to the time limit of this project, but it showed a significant difference in tolerance to the AFB1 that was consistent with results from the MTT assay.

This is the first study attempting to give direct evidence between the correlation between the high incidence of the R249S mutation in HCC tumors in the same areas with high aflatoxin exposure. Further research should be encouraged as the impacts of AFB1 on HCC carcinogenesis is a complex picture and an important field of science that needs more research.

Abbreviations

AFB1	Aflatoxin B1
AFBO	AFB1-exo-8,9-epoxide
bp	base pairs
cfDNA	circulating free deoxyribonucleic acid
DMEM	Dulbecco's Modified Eagle Medium
DMSO	Dimethyl Sulfoxide
DNA	Deoxyribonucleic acid
ED25%	Effective dose that cause 25 % death of the cell population
FCS	Fetal Calf Serum
gDNA	genomic deoxyribonucleic acid
GOF	Gain Of Function
H_2O_2	Hydrogen peroxide
HCC	Hepatocellular Carcinoma
HCl	Hydrochloric acid
LTA	Long-term treatment assay
MTT	3-(4,5-dimethylthizol-2-yl)-2,5-diphenyltetrazolium bromide
PBS	Phosphate Buffered Saline
PCR	Polymerase Chain Reaction
RFLP	Restriction Fragment Length Polymorphism
TAE	Tris-Acetate-EDTA
TP53	Tumor Protein 53

Table of content

1 Introduction

1.1 Context

The research theme "Hepatitis B infection and liver cancer" of the Pole 7, led by Prof. Emmanuelle Gormally, has historically been developed with numerous collaborations with Mali. Indeed, even today, the incidence of liver cancers is very disparate, with many cases diagnosed in West Africa. In most cases, these cancers are due to infection with the hepatitis B or C virus and/or to exposure to a mycotoxin, the aflatoxin.

I have joined Fanny Odet's project of research focusing on studying the impact of aflatoxin and more specifically aflatoxin B1 (AFB1) as a genotoxic compound leading to hepatocellular carcinoma (HCC) possibly caused by the mutation of *TP53* gene.

Therefore, first we will describe mycotoxins and explain how these, and specifically AFB1, cause a major health threat. Then we will move on to explain how AFB1, a known carcinogen, is involved in HCC and exerts its carcinogenic and genotoxic abilities. Lastly, we will explain how one of these specific genotoxic effects is the creation of mutations on the *TP53* gene, most often on the hotspot R249.

1.2 Mycotoxins

1.2.1 Origin of the mycotoxins

Mycotoxins are naturally occurring secondary metabolites produced by microfungi that frequently contaminate foods and feeds. These have the ability to cause disease and deaths in both humans and animals (Bennett & Klich, 2003). One fungus that produces such substances is the fungus *Aspergillus flavus* (*A. flavus*), a saprophytic soil fungus that is viewed as an opportunistic pathogen because of this production (Figure 1). It can be found in a variety of climate zones, but it thrives in warmer climate between latitudes 16° and 35°, and rarely above 45° latitudes (Amaike & Keller, 2011).

Mycotoxins infect both food and feed before and after harvest (Figure 1). The rate of infection is enhanced by damage created by insects and birds, as this creates entry sites. Postharvest contamination can occur as a response to poor storage procedures, such as moisture control (Amaike & Keller, 2011).

Figure 1: Aspergillus flavus and infected crop. Left: Aspergillus flavus under the microscope, a saprophytic soil fungus that is viewed as an opportunistic pathogen. (Aspergillus Flavus under Microscope | Medical Laboratories, n.d.) Right: Mycotoxin infected maize cob, postharvest contamination can occur as a response to poor storage procedures. ("Genetic Engineering and Gene Silencing Could Fight Deadly Crop Mycotoxins—If Not Blocked by Activists," 2017)

Mycotoxins are viewed as a major health problem worldwide due to the adverse health effects it causes. Dietary intake can lead to mycotoxicosis, which is frequent in under-developed countries. In addition, mycotoxins have been demonstrated to be carcinogenic, teratogenic, immunosuppressive and have mutagenic effects in humans and animal (Bennett & Klich, 2003).

There are a lot of different mycotoxins, but one of the major and most common mycotoxin is aflatoxins, produced by *A.flavus*. Over 4,5 billion people worldwide are exposed to unmonitored levels of aflatoxins, making it a global health concern (Alshannaq et al., 2018). The aflatoxin constitutes a family of over 20 different aflatoxins that carries adverse health effects. Of all the members of the aflatoxin family, aflatoxin B1 (AFB1) is the most common and toxic aflatoxin. International Agency for Research on Cancer (IARC) has classified AFB1 as a carcinogen group 1, concluding it is carcinogenic to humans (*List of Classifications – IARC Monographs on the Identification of Carcinogenic Hazards to Humans*, n.d.)

1.2.2 AFB1 and cancers

Aflatoxin B1 is associated with a number of severe chronic diseases due to long-term exposure to low concentrations of AFB1, but primarily cancer. Although their carcinogenicity is first and foremost associated with the liver where they are first metabolized, it has been demontrated in other organs including the kidney, the bladder, bone, the pancreas, central nervous system, viscera, etc., through experiments on poultry with contaminated feed (Fouad et al., 2019). It has

also been reported that inhalation of mycotoxins have developed lung cancer (Kelly et al., 1997) and that direct contact has caused skin occupational cancers (Marchese et al., 2018).

The strong correlation between AFB1 and liver cancer has been the objective to epidemiologic studies and toxicity models on animal studies. Liu and Wu have proven that there is a direct correlation between AFB1 exposure and incidence of HCC, stating that between 4,6 % and 28,2 % of all HCC cases worldwide can be attributed to aflatoxin exposure. Of these, an estimate of 40 % live in sub-Saharan Africa (Figure 2) (Liu & Wu, 2010). IARC has summarized the findings of toxicity models on animal studies, showcasing the carcinogenic severity aflatoxin has by the development of several different cancer types across all the animals that were infected (IARC, n.d.)
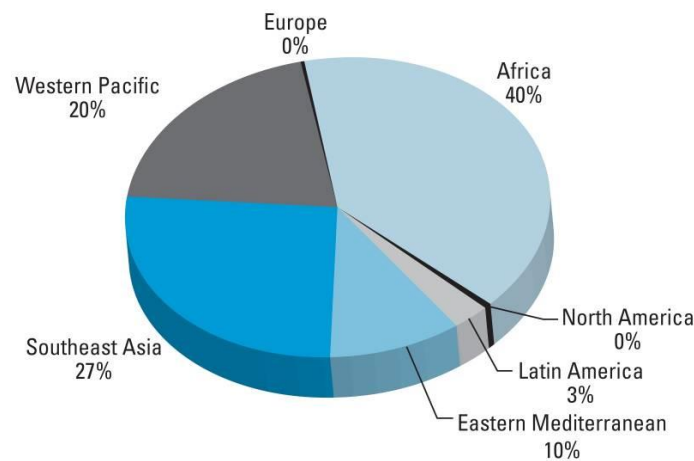
Figure 2: Global distribution of HCC cases related to AFB1 exposure. Sub-Saharan Africa is the most important region for HCC cases related to AFB1 exposure, with Western Pacific and Southeast Asia as other key regions with aflatoxin as risk factor. Europe, the Americas and Eastern Mediterranean have relatively fewer cases. (Liu & Wu, 2010)

Exposure to AFB1 causes different mechanisms involved in cancer development by exerting genotoxicity, acute toxicity and immunotoxicity. Since its discovery, the mutagenicity of AFB1 has been the most studied. Due to the highly unstable intermediate metabolite AFB1-exo-8,9-epoxide (AFBO), various metabolic, signalling, genetic and cell structure disruptions occur by the aflatoxins interraction with cellular macromolecules such as nucleic acids, proteins and phospholipids (Figure 3). Since AFB1 is metabolized in the liver, AFBO will exert its adverse abilities in this organ first. More studies suggest that the aflatoxin has equally dramatic, or even higher, effects on cell function and integrity through its capability to induce oxidative stress (Benkerroum, 2020).
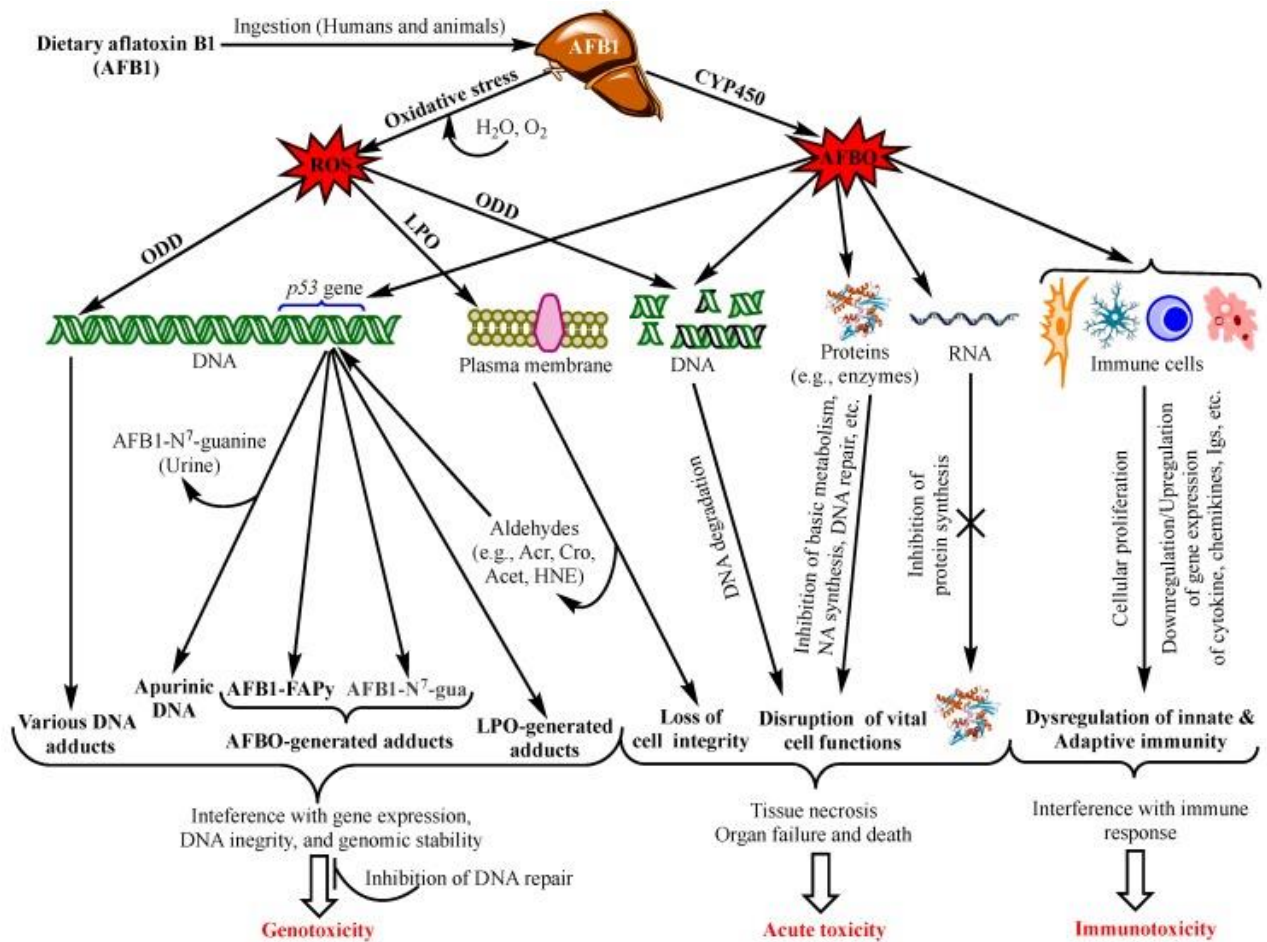
Figure 3: The main mechanisms on how AFB1 causes genotoxicity, acute toxicity and immunotoxicity through its metabolite Aflatoxin B1-exo-8,9-epoxide and oxidative stress. "NB: ROS also affect protein, RNA molecules, and immunity as does AFBO (not shown in the figure). Abbreviations: AFBO: Aflatoxin B1-exo-8,9-epoxide; NA: Nucleic Acids; ROS: Reactive Oxygen Species; LPO: Lipid Peroxidation; ODD: Oxidative DNA Damage, Acr: Acrolein; Cro: Crotonaldehyde; Acet: Acetaldehyde; HNE: 4-Hydroxy-2-Nonebal;[...]; Igs: Immunoglobulins."(Benkerroum, 2020)

At some point we will focus on the genotoxic effects of this metabolite.

1.3 AFB1 and hepatocellular carcinoma

Hepatocellular carcinoma is the predominant type of primary liver cancer, and is one of the most frequent and malignant cancer types. It ranks as the third most deadly type of cancer with an estimate of 560 000 newly diagnosed cases each year. This disease is less common, but increasing, in Western-developed countries with an incidence of 2,8-6,1 (Caucausian, African-American respectively) per 100 000, and is endemic in countries such as China, Korea, Taiwan and Sub-Saharan Africa, where the incidence can reach up to 100 cases per 100 000. The

mortality that follows HCC in these countries makes it the leading cause of cancer-related deaths, with less than 3 % of HCC patients surviving more than 5 years after being diagnosed (Hussain et al., 2007). This, and factors such as tumor recurrence, treatment resistance, drugs with modest efficiancy and being hard to diagnose early, advocate for how HCC is viewed as a major public health concern and deserve medical attention (Lee et al., 2022; Wang & Wei, 2020).

Dietary intake of low doses of aflatoxins over a longer time period has been strongly associated with development of primary liver cancer, e.g. HCC. This is the most frequent and malignant type of cancer that AFB1 has a strong correlation to. Risk factors, such as infection with hepatitis B virus (HBV), has shown to enhance the effect of AFB1 (Benkerroum, 2020).

1.3.1 Metabolism in hepatocytes

Once ingested, the aflatoxin will be absorbed in the duodenum and transported to the liver, where it will be bioactivated by CYP450, a superfamily of enzymes that function as monooxygenases. The enzymes will catalyse the oxidation of the double bond between C^8 and C^9 in the furan ring, thereby creating the two stereoisomers AFB1-exo and -endo-8,9-epoxide, where the former is considered more reactive and toxic than the other (Benkerroum, 2020).

1.3.2 AFB1 mechanisms inducing genotoxic effects

The stereoisomers of the metabolized aflatoxin are released and the endo-isomer will contribute little to the toxicity of AFB1, while the AFBO will contribute largely. The AFBO will intercalate the DNA and bind covalently to the N^7 atom of guanine residue by alkylation reaction, thereby creating the stereospecific aflatoxin-DNA adduct *trans*-8,9-dihydro-8-(N^7-guanyl)-9-hydroxy-AFB1 (AFB1-N^7-gua). The positive charge of the AFB1-N^7-gua causes it to be highly unstable, and will release itself to create more stable molecules, leaving an apurinic DNA molecule behind. More stable molecules are established under slightly alkaline conditions, where the imidazole ring may be opened. That creates the isomers *cis-* and *trans-*AFB1-formamidoprymidine (AFB1-FAPy) adducts which are both stable, called minor and major, respectively (Figure 4). The main precursors to the AFB1's genotoxic and carcinogenic effects are known to be these three (apurinic DNA, AFB1-N^7-gua and AFB1-FAPy). The most mutagenic of them is the latter due to the DNA damage it causes. This has been described to be less helix-distorting compared to the damage created by AFB1-N^7-gua, thereby making the

mutations harder to detect and be repaired by the nucleotide excision repair (NER) (Benkerroum, 2020).
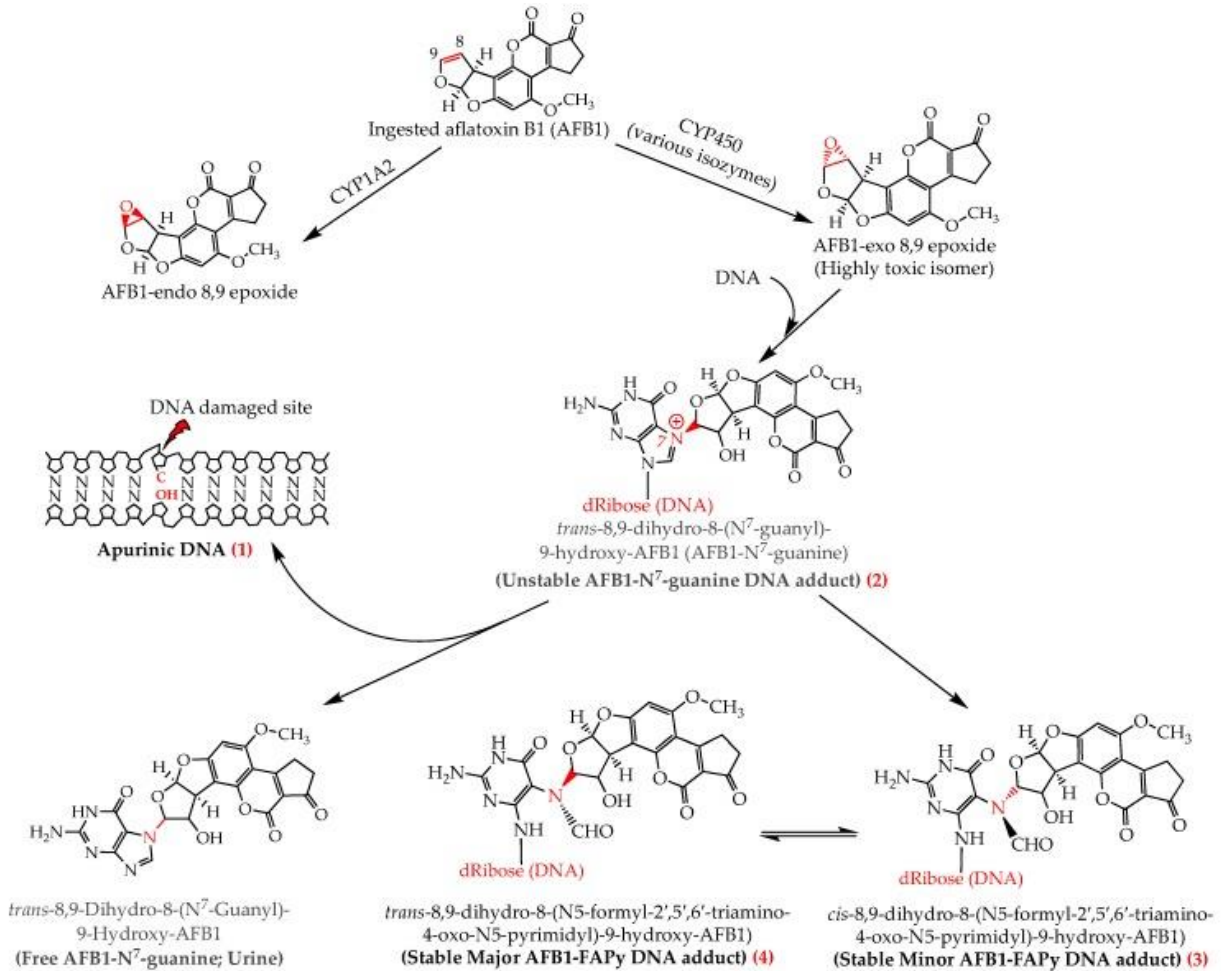
Figure 4: Bioactivation of AFB1 to its metabolites, where the toxic AFBO intercalates with DNA and creates unstable aflatoxin DNA adducts that will cause three main DNA lesions: apurinic DNA, AFB1-N7-gua and AFB1-FAPy. AFBO will intercalate the DNA to create the highly unstable AFB1-N7-guanine DNA adduct (2). The positive charge will cause it to release itself to form more stable products, leaving apurinic DNA (1) behind. Alkaline conditions are required to open the furan ring and create the stable isomers minor AFB1-FAPy (3) and major AFB1-FAPy (4) DNA adduct. (Benkerroum, 2020)

Several studies have discovered that cancers caused by AFB1 exposure have a specific mutational profile, called a mutational signature. It is the COSMIC mutational signature 24 called SBS24 (single base substitution), and has a majority of the transversions from G>T (*COSMIC | SBS - Mutational Signatures*, n.d.), which is a specific substitution where a purine is exchanged with a pyrimidine due to the covalently bound DNA adducts. This signature has been validated by Huang et al in 2017 both in vitro and in animal models (Huang et al., 2017).

The genotoxic effect of AFBO leads to the formation of DNA adducts that cause DNA damage, where one of the specific targets can be the *TP53* gene. A study in 1991 performed by Hsu et al analysed 16 HCC samples from patients in Qidong, an area in China with high incidence. This is an area where aflatoxin exposure and HBV are risk factors to this cancer type. Of these 16 tumors DNA samples, eight showed a missense mutation at the third bp of codon 249 at the *TP53* gene, where seven of these were a G>T substitution. As AFB1 is a risk factor for HCC in Qidong, the observation of this specific substitution was concluded to have aetiological implications (Hsu et al., 1991).

1.4   Tumor protein P53

Tumor protein P53 has an important role in various cell signalling pathways, especially the induction of cell cycle arrest and apoptosis, and will preserve the integrity of DNA in response to harmful stimuli.

1.4.1   Description of *TP53* gene

The *TP53* gene is located on chromosome 17 and encodes the phosphoprotein called p53. The gene spans 20 kb which includes 11 exons, though the first is noncoding. This gene does not contain a TATA box, but is under the control of several other ubiquitous transcription factors that control its expression (Schwab, 2017). *TP53* mutations in humans are most often (85-90 %) missense mutations, creating synthesis of full-length functioning proteins with a substitution. These mutations are often concentrated to the exons expressing the DNA-binding domain, creating proteins that control the same biological pathways, but with opposite effect. Mutation in the *TP53* gene is found in over 50 % of solid tumors, even without the exposure of AFB1 (Perri et al., 2016).

p53 is organized by 393 residues in a hydrophobic central core, an acidic N-terminus and a basic C-terminus. The N-terminus is made up by two complementary transcriptional activation domains, one major at residues 1-42 and the minor one at 55-75, the latter being involved in regulation of different proapoptotic genes. The C-terminus is found at residues 325-366 and contains both the main nuclear localization signals and the domain for oligomerization which is essential for transcriptional activity. Multiple regulatory functions have been connected to

the extreme C-terminus, which acts as a negative control on sequence-specific DNA-binding activities. Post-translational modification sites have also been found in both the N- and C-terminal regions (Schwab, 2017).

The central core binds to the DNA on the protein residues 102-292 (*BLAST*, n.d.). It resembles an immunoglobulin-like β-sandwich as it is made of two β-sheets stacked on top of each other that supports a set of flexible loops and helices, the loop L1 and the two bigger loops L2 and L3, which in turn are stabilized through the tetrahedrally binding of a zinc ion (Menendez et al., 2018). It is these loops and helices that are in direct contact with DNA sequences that contain inverted repeats of the sequence RRRC (A/T) (Schwab, 2017).

1.4.2   Normal function of p53

It is well-known that p53 is involved in a great number of important intracellular pathways including cell survival, DNA repair, apoptosis and senescence. Recent studies show that p53 exerts other biological functions, such as regulation of energy metabolism and anti-oxidant defence (Figure 5). The regulation of energy metabolism includes glycolysis, pentose phosphate pathway, nucleotides metabolism and others. Murine double minutes2 (MdM2) and phosphatase and tensin homolog (PTEN) is negative regulators of p53 and will inactivate the protein in un-stressed conditions (Perri et al., 2016).

One of the most understood cell signalling pathways in which p53 is important is the cell-cycle control mechanism that operates at the G_1-to-S transition. DNA damage that occurs in the G_1 will cause an increase in the concentration as well as the activity of the p53 protein, which functions as a transcription regulator that activates the gene encoding protein p21, which is encoded by the gene WAF and act as an inhibitor for cyclin-dependent protein kinases (Cdk). The protein will bind to G_1/S-Cdk and S-Cdk, both which are Cdks initiating S-phase, thereby creating a complex that inactivates them and keeps them from driving the cell into S phase, by favoring entrance to G0 phase. This gives the cell the opportunity to repair the damage done to the DNA by activation of the Growth Arrest and DNA Damage (GADD45) and p53 inducible ribonucleotide reductase (P53R2) genes, promoted by p53. If the DNA damage is too severe the p53 protein will induce genes involved in apoptosis (Alberts et al., 2019; Perri et al., 2016).
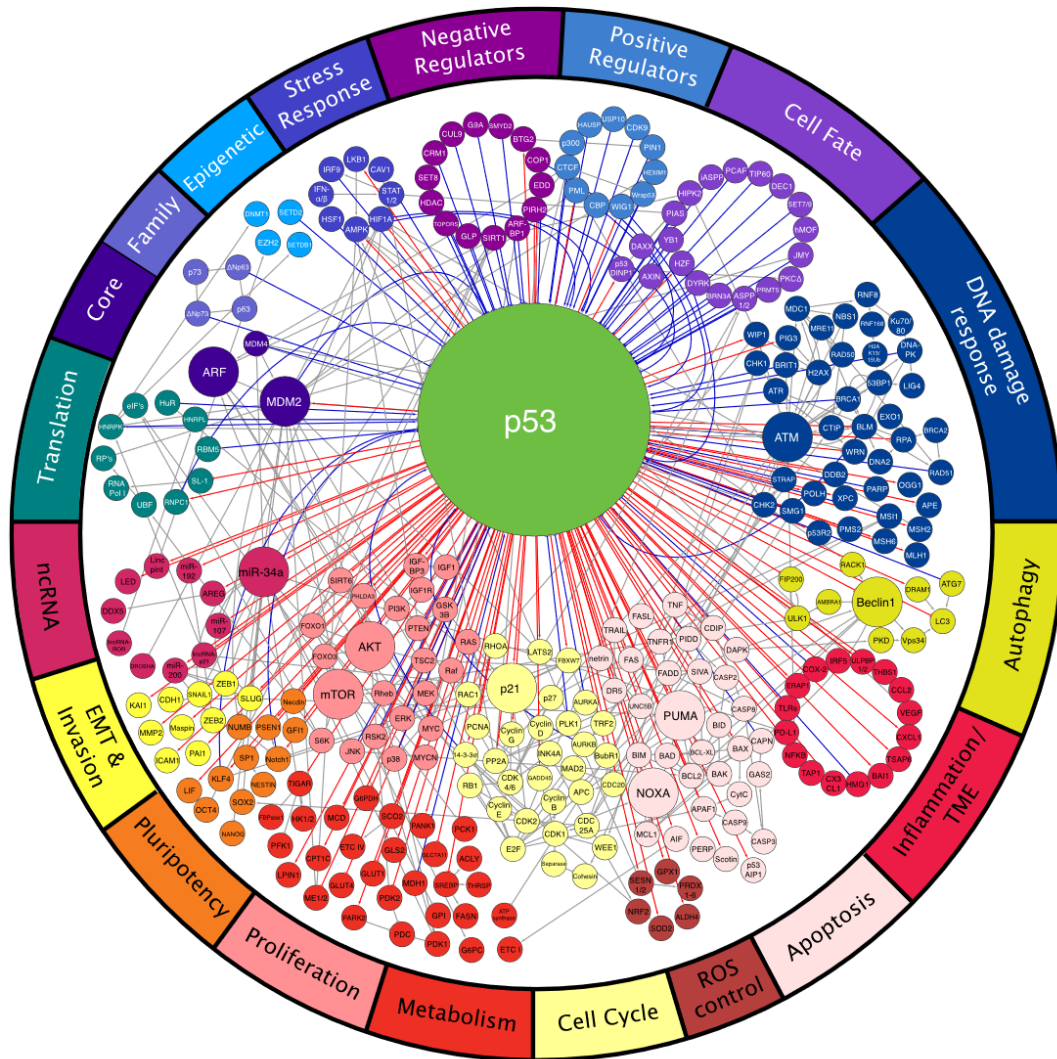
Figure 5: p53 is involved in a great number of important intracellular pathways. The well-known include apoptosis, senescence, DNA repair and cell cycle arrest. *However, recent studies have shown that p53 is also a regulator of energy metabolism and important in the defence of oxidative stress. (Kastenhuber & Lowe, 2017)*

1.4.3   Mutation hotspots in *Tp53* gene

p53 is highly responsible for preventing tumorigenesis by being an important part of the cell cycle control panel, where it can control the cell growth by temporarily halting the cell cycle or even induce apoptosis or senescence. Cancer cells have developed several tactics to disarm this protein that is so detrimental to their growth, where the most effective method is to mutate the *TP53*-gene itself, so the protein is inactivated. This leads the *TP53* gene to be highly mutated in approximately 50 % of all human cancer and thus also the most frequently mutated gene in human cancers (Figure 6) (Zhou et al., 2019). This will undoubtedly happen at multiple residues with different frequencies, where the most frequently mutated residues are called hotspots.
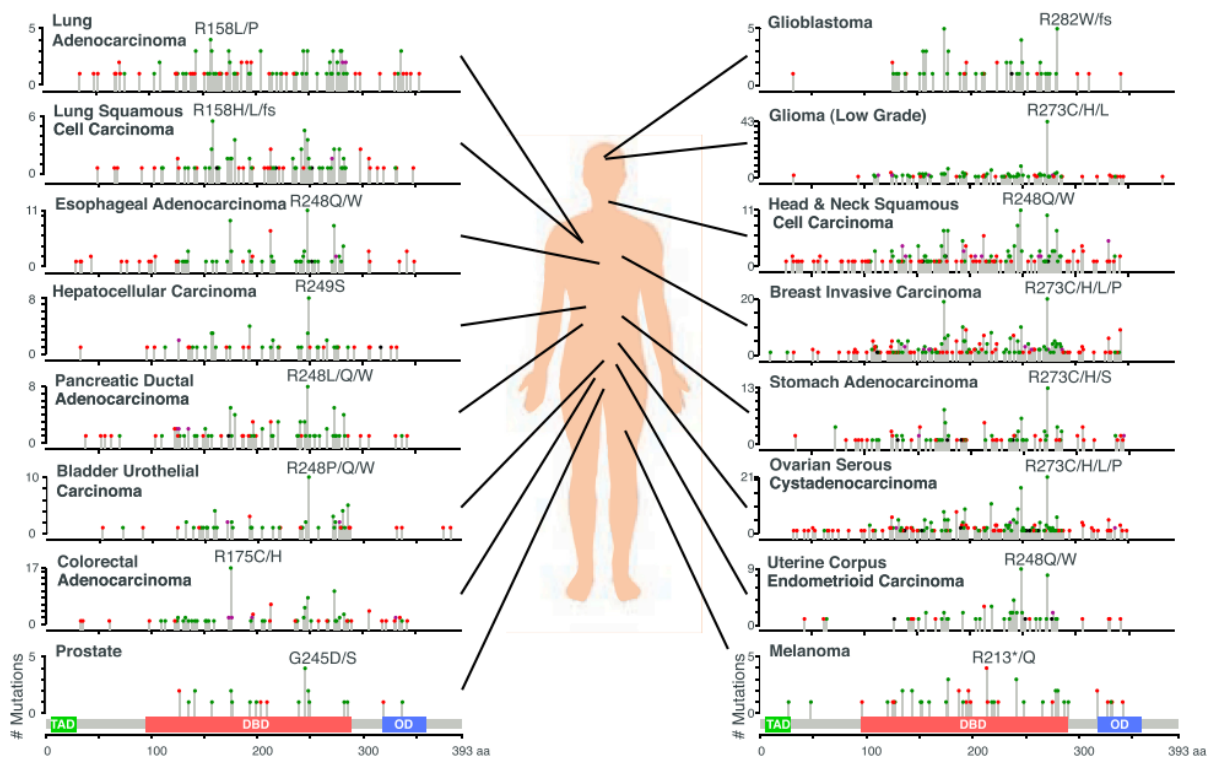
Figure 6: TP53 is the most frequently mutated gene in all human cancers. The figure depicts the different hotspots on p53 for different types of cancers across different parts of the body. The R249S mutation is the most frequent for hepatocellular carcinoma. (Kastenhuber & Lowe, 2017)

The most frequent mutation type of *TP53* is missense which counts for approximately 85-90 % (Perri et al., 2016), a single substitution of nucleotide that leads to a change in the encoded amino acid. Other types of mutations are also included; frameshift, truncation and deletion mutations are among these. Among 80 % of the missense mutations occur in the DNA-binding domain and several hotspots have been identified, including R175, Y220, G245, R248, R249, R273 and R282. The p53 mutants can be grouped into two categories, DNA-contact mutants where the mutant itself replaces the amino acid that is critical for binding the DNA, and conformational mutants that leads to unfolded structure or altered conformations. Among the latter the mutation R249S is found, which in addition to having altered conformation also find itself in the minority of mutations that acquire "gain-of-functions" (GOF) which will highly promote carcinogenesis, while the majority of p53 mutants will lose the wild-type function. (Zhou et al., 2019)

Mutations such as R249S are both unable to bind specifically to the original DNA elements and obtain a GOF activity that is essential for the growth and survival of cancer cells. These GOF activities are generally executed through molecular mechanisms, such as "uncontrolled" cell proliferation and promotion of invasion and metastasis. The GOF activity of a HCC specific p53 mutant, R249S, has been revealed and the mechanism is unique as it recruits other oncoproteins to execute the mutant's activity (Figure 7). The p53-R249S is firstly phosphorylated at the cancer-derived serine 249 by a complex of cyclin-dependent kinase 4 and cyclin D1 (CDK4/CycD1) before interacting with peptidylprolyl *cis/trans* isomerase, NIMA-interacting 1 protein (PIN1) to facilitate the import of the phosphorylated molecule to the nucleus. Once there, MYC proto-oncogene, bHLH transcription factor (c-MYC) will bind to the molecule thus becoming more active and boosts the transcription of the targeted genes involved in ribosomal biogenesis. This will consequently enhance the survival and proliferation of the HCC, thus making this p53 mutant HCC-specific (Zhou et al., 2019).
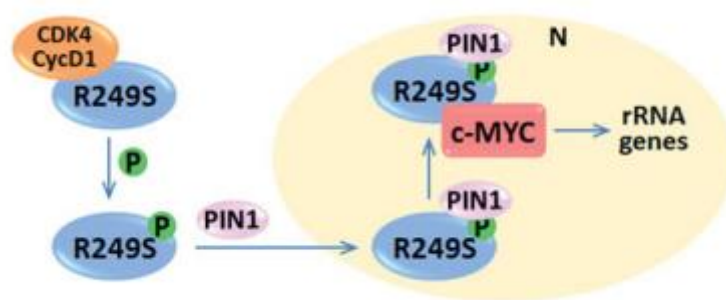
Figure 7: The p53 mutant R249S has a unique mechanism that enhance survival and proliferation of HCC. A complex of cyclin-dependent kinase 4 and cyclin D1 (CDK4/CycD1) phosphorylates the molecule at serine 249. The phosphorylated molecule interacts with peptidylprolyl cis/trans isomerase, NIMA-interacting 1 protein (PIN1) which facilitates the nuclear import. Once there MYC proto-oncogene, bHLH transcription factor (c-MYC) binds to the molecule, boosting the activity and transcription of the targeted genes. (Zhou et al., 2019)

The R249S mutation is detected in more than 60 % of patients with HCC and is present in 75 % of Chinese and 56 % of Mozambican Shnagaans HCC tumor tissue, showing a correlation between hotspot 249 and HCC incidence. The G>T transversion accounts for 90 % of the AFB1-related mutations on the *TP53* gene (Kew, 2013), where the R249S mutation is dominating in Western Pacific, Southeast Asia, and Sub-Saharan Africa (Figure 8) (Hussain et al., 2007).
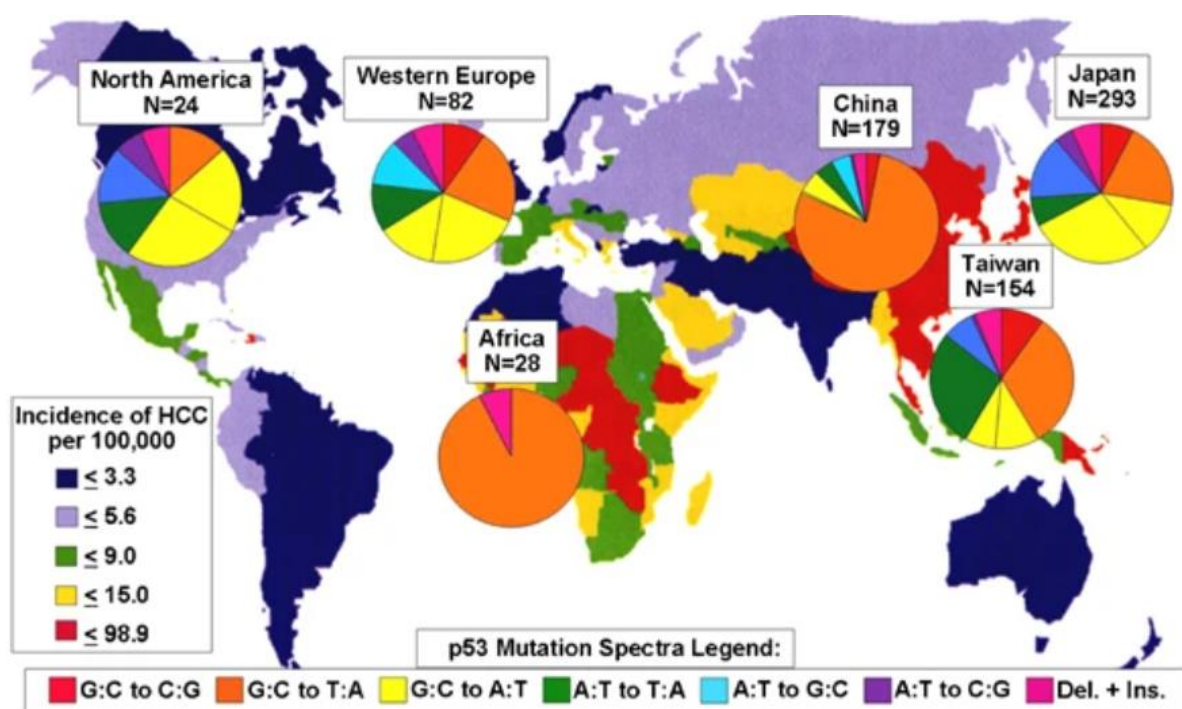
Figure 8: Global distribution of incidence of HCC with pie diagrams of distribution of TP53 mutations in key countries and continents. G>T transversion is dominating in areas of dietary AFB1 exposure and endemic HBV infection. (Hussain et al., 2007)

1.5 Objective

1.5.1 AFB1, direct cause of the site-specific mutation?

Over the years there have been multiple epidemiologic studies showing the strong and direct correlation between geographically areas with high incidence of HCC and areas with high incidence of AFB1 exposure, as well as published articles covering experiments showing direct evidence that AFB1 exposure leads to a higher mutation frequency. However, to our knowledge it is yet to be published research showing real direct evidence between AFB1 exposure and the creation of R249S mutation as a response mechanism. This suggest that the published epidemiologic studies reside heavily on correlation without using direct studies between AFB1 and the mutation as evidence.

Kew stated in a review of 2013 when discussing the R249S mutation *"[...] suggesting that its presence confers a selective advantage during hepatocarcinogenesis"* (Kew, 2013), but to our knowledge no real direct evidence was established. In another study, Huang et al stated *"The prevalence of the TP53 R249S mutation in HCCs with combined hepatitis B and aflatoxin exposure is remarkable, but the sensitivity of R249S as an indicator of aflatoxin exposure has*

been difficult to study systematically.[…] This makes it difficult to assess the strength of the association between the R249S mutation and long-term aflatoxin exposure (Groopman et al. 1985; Wild et al. 1986; Egner et al. 2006)" (Huang et al., 2017). This validates our assumption that this association has not been proven before.

1.5.2 Hypothesis

The hypothesis is that when the cells in vivo are exposed to AFB1 all kinds of mutations will occur, and for some cells this mutation will be the R249S for p53. This specific mutation would give a selective and proliferative advantage which will end up with a tumor consisting of cells with the R249S mutation.

To determine if AFB1 have a direct impact on inducing this specific mutation linked to HCC, we want to explore two questions using cellular models:

1) *Will either the absence or the mutation of TP53 favor cell survival during an AFB1 treatment using different cell lines with different TP53 statuses?*

2) *Will a long-term treatment with AFB1 (more than 45 days) on a cell line possessing non-mutated TP53 induce the R249S mutation?*
   a. *And if so, will the mutated clones take over the culture, thereby proving a selective advantage of the altered cells?*

2   Material and methods

2.1   Description of the different cell lines used as models

For this project six different cell lines with different *TP53* profiles were available and used.

***Tp53* non-mutated hepatocyte-derived cell line**

HepG2: immortalized cell line derived from the liver tissue of a 15 year-old Caucasian male who had a well-differentiated hepatocellular carcinoma (Aden et al., 1979).

Cell line with Y220C-mutated form and overexpression of *TP53*

HuH7: cell line derived from the liver tissue of a 57 year-old Asian male with hepatocellular carcinoma (Nakabayashi et al., 1982). The mutation at codon 220 on the *TP53* gene causes this cell line to overexpress p53 (Papachristou et al., 2021).

Cell lines with R249S-mutated form of *TP53*

Mahlavu: cell line derived from the liver tissue of an African female with hepatocellular carcinoma. This cell line is infected with the hepatitis B virus and has the R249S mutation on the *TP53* gene (*Liver Cancer Cell Lines Database*, n.d.-a).

PLC/PRF/5: cell line derived from the liver tissue of a 24 year-old African male with hepatocellular carcinoma. This cell line is infected with the hepatitis B virus and has the R249S mutation on the *TP53* gene (*Liver Cancer Cell Lines Database*, n.d.-b).

Cell lines with invalidation on both alleles of *TP53* gene

Hep3B: cell line derived from the liver tissue of an 8 year-old African-American male who had a well-differentiated hepatocellular carcinoma (Aden et al., 1979). These cells have an integrated hepatitis B virus genome (*Hep 3B2.1-7 [Hep 3B, Hep-3B, Hep3B] | ATCC*, n.d.).

Embryonic kidney-derived cell line

293T: cell line derived from the kidney tissue of a foetus (*293T | ATCC*, n.d.).

All cell lines were cultured during the entire project, but operational errors caused us to periodically lose some of the cell lines. Due to this, and the fact that this project was too limited in time, our experiments focused on the most stable cell lines causing us to only present data on HepG2, HuH7 and Mahlavu.

2.2   Cell maintenance

Practical work regarding the cell culture was performed under aseptic conditions under a biosafety hood and cell cultures were incubated in a humidified atmosphere of 5 % CO_2 – 95 % air at 37°C.

Medium for cell culture was made by supplementing High Glucose DMEM (Gibco™, 61965-026) with 10 % FCS (Fetal Calf Serum, Eurobio Scientific, CVFSVF00-01), 1X MEM Non-Essential Amino-Acids (Gibco™, 11140-050), 1X Antibiotic-Antimyotic (Gibco™, 15240-062) and 1 mM Sodium Pyruvate (Gibco™, 11360-070). This is referred to as complete medium in this report.

Cell cultures were observed in a Leica-DML microscope daily and commented regarding their confluency and morphology. When the cell confluency reached 65 to 95 %, cell cultures were split approximately every 3-5 days depending on the cell line. Cell individualization was performed as followed: after discarding the old medium, the cells were washed twice with PBS without calcium or magnesium (Gibco™, 14190-144). Trypsin 1X (1 mL) (0,05 %, Gibco™, 25300-054) was added and the cells were incubated in 37°C (5 % CO_2) for 5 minutes. After mechanical individualization of the cells by gently pipetting up and down, trypsin activation was inhibited by adding complete medium (4 to 8 mL). Cell suspensions were homogenized using a Corning® Stripettor™ Ultra pipet.

An aliquot of this cell suspension was counted using a Malassez counting chamber, where the cell count in each line corresponds to 0,1 µL total. Cell suspensions was diluted in half with Trypan Blue Stain (0,4 %, Gibco™, 15250-061) to label dead cells exclusively in blue. The concentration of viable cells was calculated following formulas 1-3.

$$Cell\ concentration\ \left(\frac{cell\ number}{mL}\right) \atop = average\ cell\ count\ in\ one\ line * dilution\ factor * 10^4 \tag{1}$$

$$Total\ quantity\ of\ cells = cell\ concentration * total\ volume\ cell\ suspension \tag{2}$$

$$\%\ cell\ viability = 100\ \% - \left(\frac{total\ dead\ cells\ count}{total\ cells\ count} * 100\ \%\right) \tag{3}$$

For cell maintenance, the number of cells seeded depended on the cell line, as shown in Table 1. The cell cultures were seeded in new Petri dishes with desired cell concentration with estimated volume of both cell suspension and new complete medium, based on the result and

the need of cells. The new Petri dishes were labelled with cell line, date, passage, initials, and total cell count, and incubated at 37°C (5 % CO_2).

Table 1: Number of viable cells seeded for the different cell lines in 100mm diameter Petri dishes.

Cell line	HepG2	HuH7	Mahlavu
Number of cells seeded	$1*10^6$	$2*10^6$	$0,5*10^6$

Hep3B needed special care and did not follow the standardized seeding. The cell line was extremely slow growing and did not grow well if they were too diluted. This led to cell maintenance to not usually include cell count, but rather use a ½ dilution. To eliminate the leftover of trypsin, cells were centrifuged at $3*1000g$ for 5 min. The cell pellet was resuspended in complete medium (20 mL); after resuspension, 2 times 10 mL of the cell suspension were in the end plated.

Only one cell line was handled at a time under the biosafety cabinet to avoid any cross-contamination. They were further used for different experiments, an overview of the applicated methods in this project is shown in Figure 9.
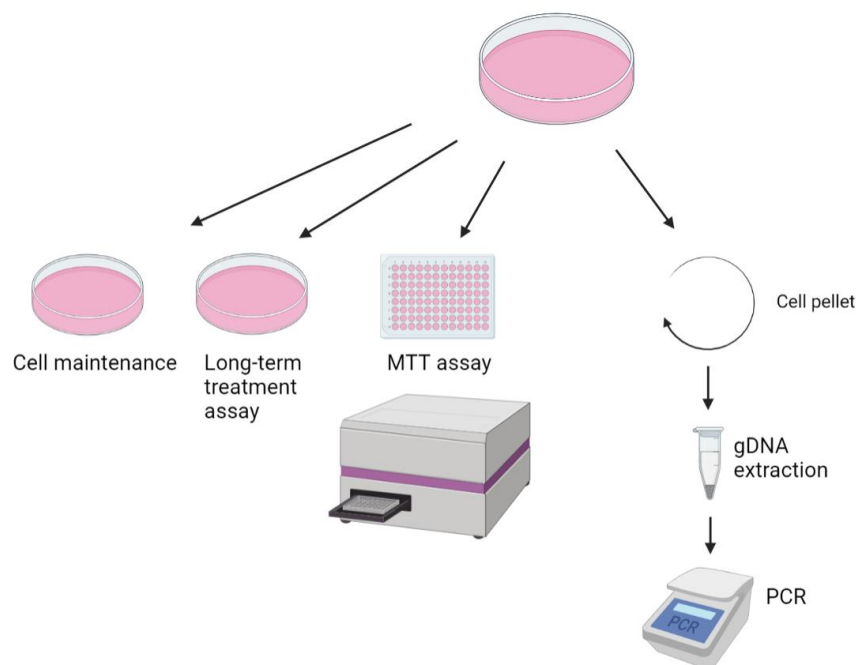

Figure 9: Overview of the applicated methods performed to investigate the hypothesis and two questions. Cell maintenance was performed to maintain the stock of material for each cell line. The performed methods include long-term treatment assay, MTT assay and gDNA extraction with PCR. Created with BioRender.com.

2.3 MTT assay as a method to follow cell viability

2.3.1 Principle of the MTT assay

The MTT assay measures cell viability by detecting absorbance, which is directly connected to the reductive activity of the mitochondrial enzymes. As the tetrazolium compound enters living cells, dehydrogenases in mitochondria reduces it to water insoluble formazan crystals, giving the sample a purple colour (Figure 10). The absorbance of the purple solution is detected spectrophotometrically and the amount of absorbance is proportional to the cell number (Mosmann, 1983).
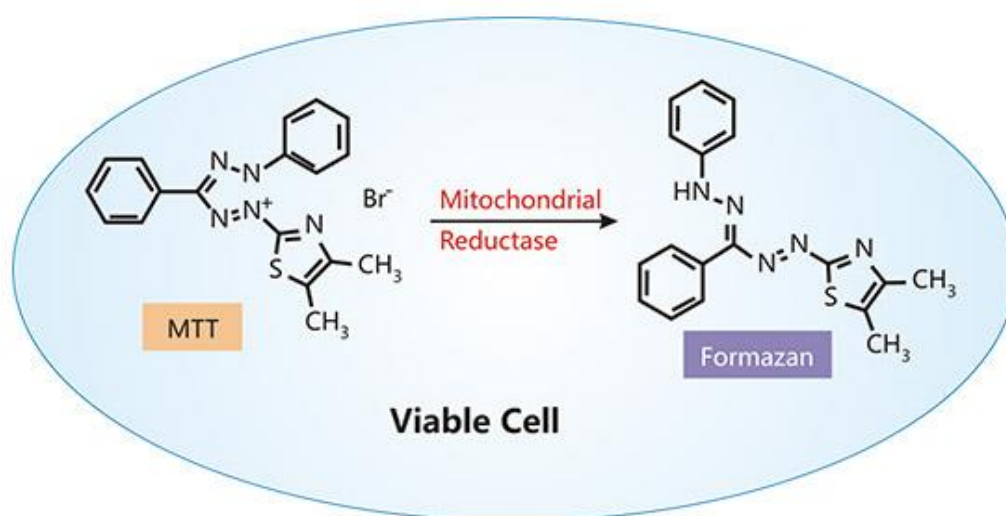
Figure 10: The MTT assay uses the mitochondrial reductive activity in viable cells to create absorbance by the creation of violet formazan crystals. *The absorbance of these insoluble crystals is detected spectrophotometrically and is proportional to the cell number. (The Overview of Cell Viability, n.d.)*

The experiment requires different steps, from seeding of cells, cells treatment to the endpoint MTT assay, so the overall experiment was designed as shown in Figure 11.
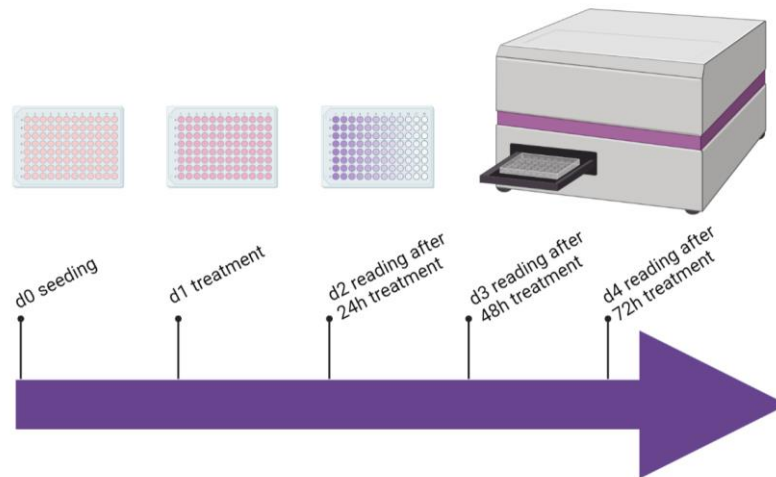
Figure 11: An overview of the setup of the MTT assay*. The seeding of the cells in 96 well plates were done on d0. The treatment with different concentrations of AFB1 was added on d1. The plates were read using a microplate reader on d2 (24h after treatment), d3 (48h after treatment) or d4 (72h after treatment). The figure shows how the MTT reagent will form violet formazan crystals on d2, d3 and d4 when adding the stop solution. Created with BioRender.com.*

2.3.2 Cell seeding

Cells used to perform the MTT assay were seeded in 96 well plates (Corning).

Different cell concentrations were tested from 2000 to 20 000 cells per well in 100 µL complete medium.

The different cell lines were plated to a 96 well plate on d0. This was done by cell trypsinization and cell count on a cell suspension from 2 or more Petri dishes. The required calculations were done to be able to have a cell suspension in complete medium at the desired cell number. After careful homogenization, cell suspension was transferred to the 96 well plate in each well using a VWR Signature Ergonomic High-Performance multichannel pipette. The plate was incubated at 37°C (5 % CO_2). Replicates of well containing the same number of cells are verified by observations with light microscopy: wells without the expected confluency were discarded from the test.

For some tests, cells were directly tested after a 2h incubation in order to let cells attach to the bottom of the well.

Cells treated with AFB1 were seeded 1 day before the treatment (day 1, d1), allowed to grow in a humidified incubator at 37°C with 5 % CO_2, and stopped 24h (d2), 48h (d3) or 72h (d4) after the treatment.

In each plate, a control line (12 wells) without cells but containing 100 µL complete medium was added to be able to measure a background "no cells".

2.3.3   AFB1 cell treatment

The water-insoluble powder of AFB1 (Aflatoxin B_1 from Aspergillus flavus, Sigma-Aldrich, A6636-5MG) was reconstituted at a 30 mM concentration in DMSO (Dimethyl Sulfoxide for cell culture, PanReac AppliChem ITW Reagents, A3672,0100). Aliquots of this AFB1 stock were made and stored in the dark at -20°C. Before treatment, the AFB1 solution was diluted in 1/3 in PBS to obtain a 10 mM AFB1 solution.

Cells were treated by diluting the 10 mM AFB1 solution in the complete medium at the desired concentration (Table 2).

Diluent controls were cells treated with the maximum amount of AFB1 diluent, meaning DMSO. When assays were treated with maximum 250 µM or 100 µM AFB1, the diluent controls received respectively 0,833 % or 0,33 % DMSO.

Table 2: The setup for the 96 well plate used for treatment optimization using different concentrations of AFB1, blanks and control with the AFB1 diluent.

Only medium / background "NO cells"
Non-treated cells
Diluent control
Cells treated with 0,01 µM AFB1
0,1 µM AFB1
1 µM AFB1
10 µM AFB1
100 µM AFB1
250 µM AFB1
Cell death positive control: cells treated with 5 to 20 % DMSO

2.3.4 MTT reagents

MTT was purchased from Sigma-Aldrich (M2003). MTT powder was resuspended in sterile PBS at 5 mg/mL. The solution was filtered and stored at -20°C, protected from light. The resolubilized MTT solution was kept only for 2 months to avoid spontaneous degradation.

Just before the MTT test, the desired volume of MTT was thawed in the dark and kept in aluminium foil.

To stop the reaction and dissolve the water-insoluble formazan, 3 different stop solutions were tested: (1) 1%SDS/0,01MHCl, (2) Isopropanol/4mMHCl/0,1%NP-40 and (3) DMSO.

2.3.5 MTT assay

Slight variations in final MTT concentration and time of incubation were done on the preliminary experiments to set up the MTT assay. However, classically, the MTT assay was performed as followed.

10 µL of the MTT solution at 5 mg/mL was added in each well containing 100 µL complete medium. Cells were incubated for 2h at 37°C (5 % CO_2). As the MTT solution is light sensitive both the reagent and the treated cells were protected from light during this part of the MTT assay.

After the incubation the excess medium was carefully discarded using a multichannel pipette and stop solution was added to each well. This was mixed thoroughly using a shaker for 10 minutes.

Then the absorbance of the 96 well plate was detected at 560 nm (primary wavelength) and 690 nm (secondary wavelength used as an internal background) using Thermo Scientific™ Varioskan™ LUX multimode microplate reader (Varioskan) (Figure 12).

The absorbances were corrected using formula 4 before being further processed:

$$Corrected\ absorbance \qquad\qquad\qquad (4)$$
$$= (Absorbance\ at\ 560\ nm$$
$$- Absorbance\ at\ 690\ nm\ as\ a\ referance\ wavelength)$$
$$- Avg\ of\ the\ absorbance\ of\ "No\ cells"\ wells\ background$$

Each condition was repeated in minimum quadruplicate in each 96 well plate.
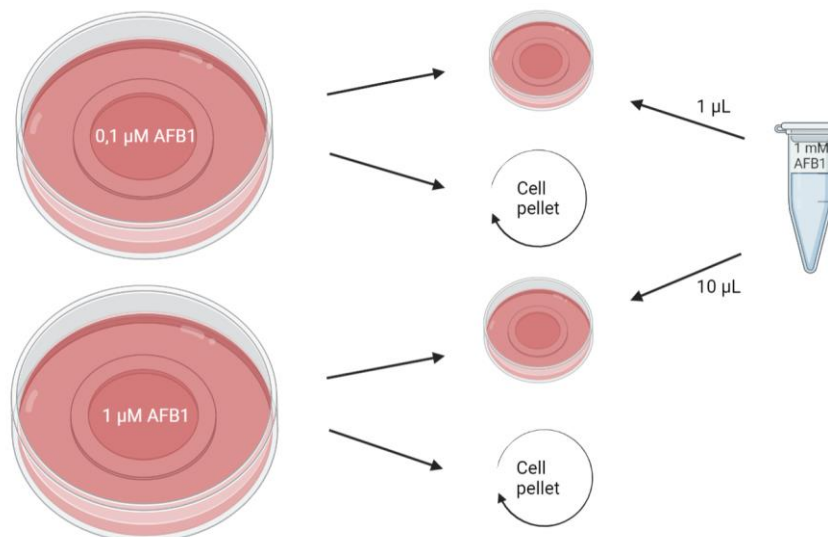
2.4 Long-term treatment assay

The long-term treatment assay (LTA) was performed using HepG2 and HuH7.

The first assay named LTA#1 was performed by seeding $1*10^6$ cells in each of the Petri dishes for each cell line, adding AFB1 (1 µL at 10 mM, solubilized 1:3 DMSO: PBS) to one Petri dish and the same volume of 33 % DMSO to the other.

The LTA#2 conditions were adjusted to 0,1 µM and 1 µM of AFB1 treatment. Cells used to do the cell maintenance were used as non-treated controls.

To perform the LTA, the pair of cell cultures with the same cell line were trypsinization and seeded to a new Petri dish each. For the standardized LTA#2, HepG2 was seeded with a cell concentration of $1*10^6$ cells /10 mL, while HuH7 was seeded with $2*10^6$ cells/mL. The Petri dish with 0,1 µM AFB1 was treated with 1 µL of AFB1 (1 mM, solubilized in 1:30 DMSO: PBS solution) while the Petri dish with 1 µM AFB1 was treated with 10 µL of the same solution (Figure 12).

Excess cell suspension was pelleted and stored at -20°C for further analysis. This treatment was repeated consistently two times a week during the period.

Figure 12: Long-term treatment assay performed on HepG2 and HuH7 with 0,1 µM and 1 µM aflatoxin B1 (AFB1) from stock solution at 1 mM. With every new passage the leftover cell suspension was pelleted and stored at -20°C for further analysis. Created with BioRender.com.

When the LTA was stopped the cells were washed and mechanically detached from the Petri dish without performing a cell count before being pelleted and saved at -20°C for further analysis.

2.5   DNA extraction and analysis to detect the presence of the R249S mutation

2.5.1   gDNA extraction

DNA extraction was performed using the Wizard® Genomic DNA Purification Kit (Promega, A1125), following the manufacturer's protocol with minor changes. Cell pellets was thoroughly resuspended in nucleic lysis (600 µL). After adding of RNase A Solution (3 µL), samples were incubated for 30 minutes at 37°C to ensure that all RNA were degraded, then the protein precipitation solution (200 µL) was added. Samples were vortexed and kept on ice for 15 min minimum. After a centrifugation at 12 000 RPM at 4°C for 4 min, supernatant containing gDNA was transferred to a new tube containing isopropanol (600 µL). After mixing by inversion, gDNA was pelleted by centrifugation at 13 000g for 1 min and washed with ethanol (70 %, 600 µL). Pellet of gDNA was air-dried and resuspended in DNA rehydration solution (150 µL). The rehydrated DNA was stored at 4°C overnight or in a freezer at -20°C before performing the DNA dosage.

2.5.2   DNA dosage using the µdrop plate

The quantity and purity of obtained gDNA was measured with a photometric assay using a µdrop plate. Using this method, rehydrated DNA (2 to 4 µL) and corresponding blank was added in each well. Upon closing the lid carefully, the plate was put in Varioskan and the assay ran as programmed. The machine's software automatically measured the absorbance spectrum between 230 nm and 330 nm, and calculated DNA dosage and -purities following the equations 5, 6 and 7.

$$gDNA\ conentration = (Abs260\ nm - Abs320\ nm) * (\frac{50}{0,049}) \tag{5}$$

$$DNA\ Purity = \frac{Abs260\ nm - Abs320\ nm}{Abs280\ nm - Abs320\ nm} \tag{6}$$

$$DNA\ Purity = \frac{Abs260\ nm - Abs320\ nm}{Abs230\ nm - Abs320\ nm} \tag{7}$$

2.5.3 RFLP

Restriction Fragment Length Polymorphism (RFLP) was used as the detection method for the R249S mutation. It is based on the fact that mutation R249S destroys a HaeIII restriction site. Therefore, digestion of wild type amplicons generates 2 visible bands of 92bp and 66bp, whereas mutant yields a band of 158 bp (Figure 13). A second HaeIII restriction site present in the PCR product provided a positive control for digestion.
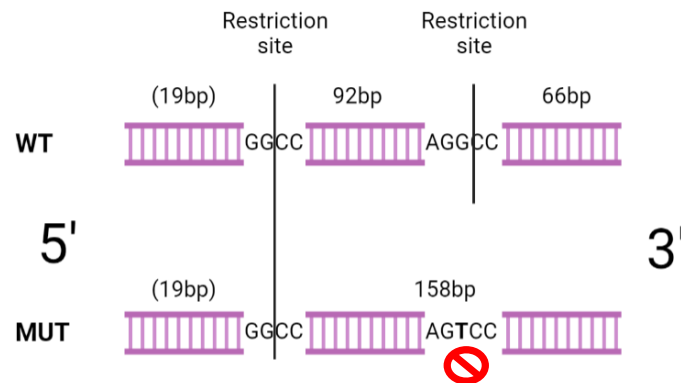
Figure 13: The R249S mutation on Tp53 gene destroys a restriction site for HaeIII. *Digestion will generate two visible bands of 92bp and 66bp for the wild type (WT), while the mutated gene (MUT) will yield a band at 158bp. Created with BioRender.com.*

2.5.3.1 PCR

PCR was performed to amplify part of exon 7 of the *Tp53* human gene flanking the R249S mutation. Primers were as followed: forward Tp53-E7(P237)-7674330-For 5' aggcgcactggcctcatctt 3', and reverse Tp5*3*-E7(P238)-7674154-Rev 5' tgtgcagggtggcaagtggc 3'. The 177bp PCR products were amplified using gDNA template (around 10 ng), each primer (0,5 µM final) and 1X PurpleTaq mastermix 2x (Thermo Scientific, EP0701). Controls without DNA template were run to monitor for possible contamination. The program was as followed: 94°C 5min; [94°C 30s, 65°C 30s, 72°C 30s] x 30 cycles; 72°C 10 min; 10°C final.

2.5.3.2 Digestion

For the digestion it was used the enzyme HaeIII (Promega, R617A), which will recognize its restriction sites, creating three DNA fragments of the wild type amplicon with the lengths 92bp, 66bp and 19bp. In case of a mutated gene on Ser249, the enzyme will not be able to cut and will result in two fragments, 158bp and 19bp. The undigested samples will remain at 177bp.

For the practical performance, HaeIII (1 µL) was mixed with each of the PCR products (10 µL). This was incubated for at least 1h. at 37°C.

2.5.3.3 Migration and analysis

An agarose gel 3 % was prepared for the migration using Agarose standard (Eurobio Scientific, GEPAGA07-62), TAE (1X) prepared by diluting a 50X Solution (Fisher BioReagents™, BP1332-500) and GelRed Nucleic Acid Stain (0,01 %) (Biotium, 41003). After the gel solution had solidified and the digestion had incubated for a sufficient time, the gel and TAE 1X as running buffer were added to an EmbiTec RunOne™ Electrophoresis Cell. Then Mid Range DNA Ladder (5 µL) (Jena Bioscience, M-203S) and digested samples (10 µL), as well as undigested PCR product as a control, were loaded to the gel. Voltage was applied until sufficient migration was obtained before using a Bio-Rad ChemiDoc™ Imaging System to detect the different bp bands in the gel.

3 Results

3.1 Cell survival

Our first question investigates if cell lines with the mutation R249S in *TP53* gene will favor cell survival and proliferation during an AFB1 treatment. A method that can be used to such is MTT assay.

Theoretically, it is a rapid, standardized, sensitive, and economical method to determine cell viability. Though this assay has been considered as a golden standard, not one common protocol was followed, and it was quickly established that this assay needed to be optimized in our laboratory.

Therefore, in preliminary experiments, different protocols were tested to establish the conditions resulting to the most reproducible results in our hands and with our cell lines.

In a second time, the cytotoxicity of AFB1 was assessed in order to determine ED25% values (Effective Dose, i.e. the concentration causing 25 % cell death).

3.1.1 Optimization of the MTT assay

Our optimization focused on three aspects: the stop solution, the cell number in each well and concentrations of the aflatoxin.

3.1.1.1 Isopropanol/4mMHCl/0,1%NP-40 is the best suited stop solution

The stop solution in MTT assay is given after a 2h incubation with the MTT reagent to stop the creation of insoluble formazan crystals and to solubilize them. Dissolving the formazan should produce a homogeneous solution suitable for measurement of optical density. Therefore, using the optimal stop solution is important to achieve a strong and accurate absorbance from the spectrophotometrically reading.

HepG2 seeded at 20 000 cells/100 µL in each well 24h in advance were used to perform the MTT assay to test three different stop solutions: (1) a convenient SDS solution (1%SDS/0,01MHCl) (Tada et al., 1986), (2) the acidified isopropanol solution (Isopropanol/4mMHCl/0,1%NP-40) (Mosmann, 1983) and (3) DMSO (Twentyman & Luscombe, 1987). These were used in different amounts and with or without carefully discarding the medium from the wells. To note, no PBS wash(es) was performed even if it was

a common protocol; indeed, risks to detach the cells and lose formazan crystals were too high, and the interference of medium containing Phenol Red was minimized with the acidic solutions.

An absorbance spectrum was performed in the range of 400-800 nm as shown in Figure 14 to determine the wavelength of maximum absorbance (Lambda Max) for each solution and for this specific microplate reader machine.
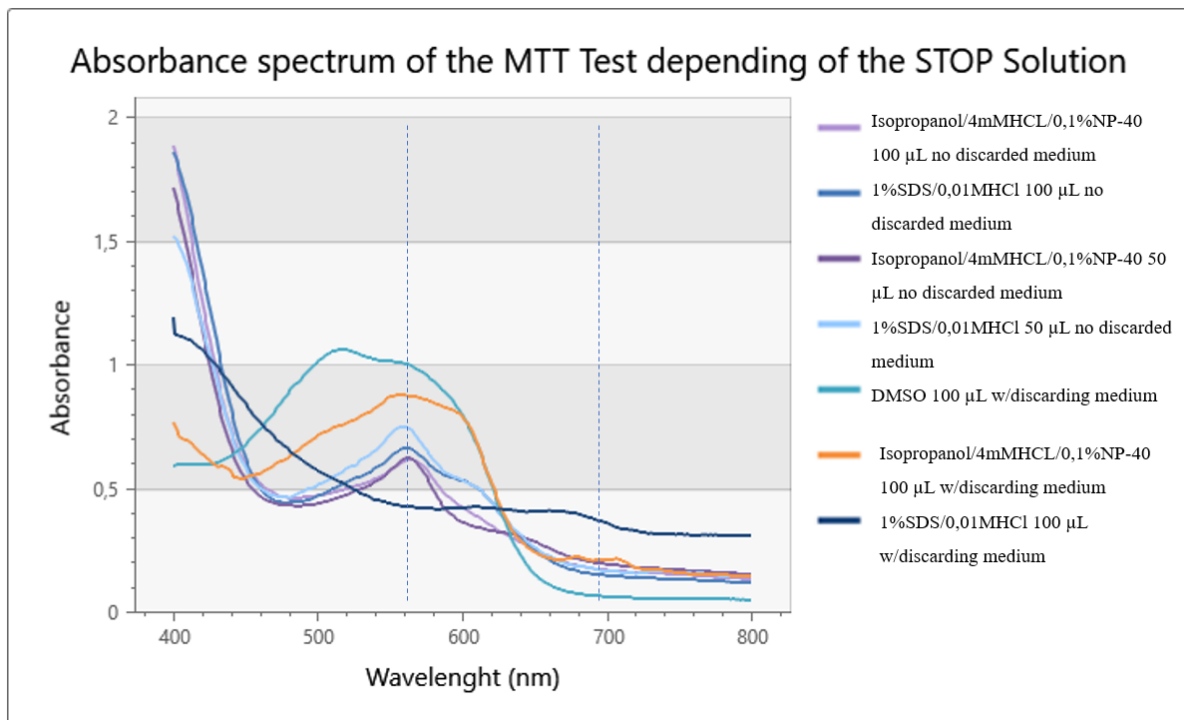

Figure 14: Absorbance spectrum in the range of 400-800 nm using the Varioskan Lux microplate reader to determine the wavelength of maximum absorbance. Different volumes and conditions for the medium were used for the three different stop solutions: 1%SDS/0,01MHCl, Isopropanol/4mMHCl/0,1%NP-40 and DMSO. The dashed lines represent the 560nm and 690 nm marks.

For all the solutions, a test wavelength of 560 nm and a reference wavelength of 690 nm were adequate. The spectrum shows that DMSO has the strongest absorbance between 500 and 600 nm, but with a very broad peak. DMSO is confirmed to be the best solvent for dissolving the formazan product (Twentyman & Luscombe, 1987), but the stop solution (2) Isopropanol/4mMHCl/0,1%NP-40 100 μL with discarding the medium showed a high absorbance without the major disadvantage of the DMSO being toxic for the experimenter and thus requiring special waste management, therefore DMSO was not chosen.

To investigate the repeatability in each well internal replicate was performed with no treated cells, corresponding to the 100 % cell viability, and cells treated with 10 % DMSO to induce cell death (Figure 15).
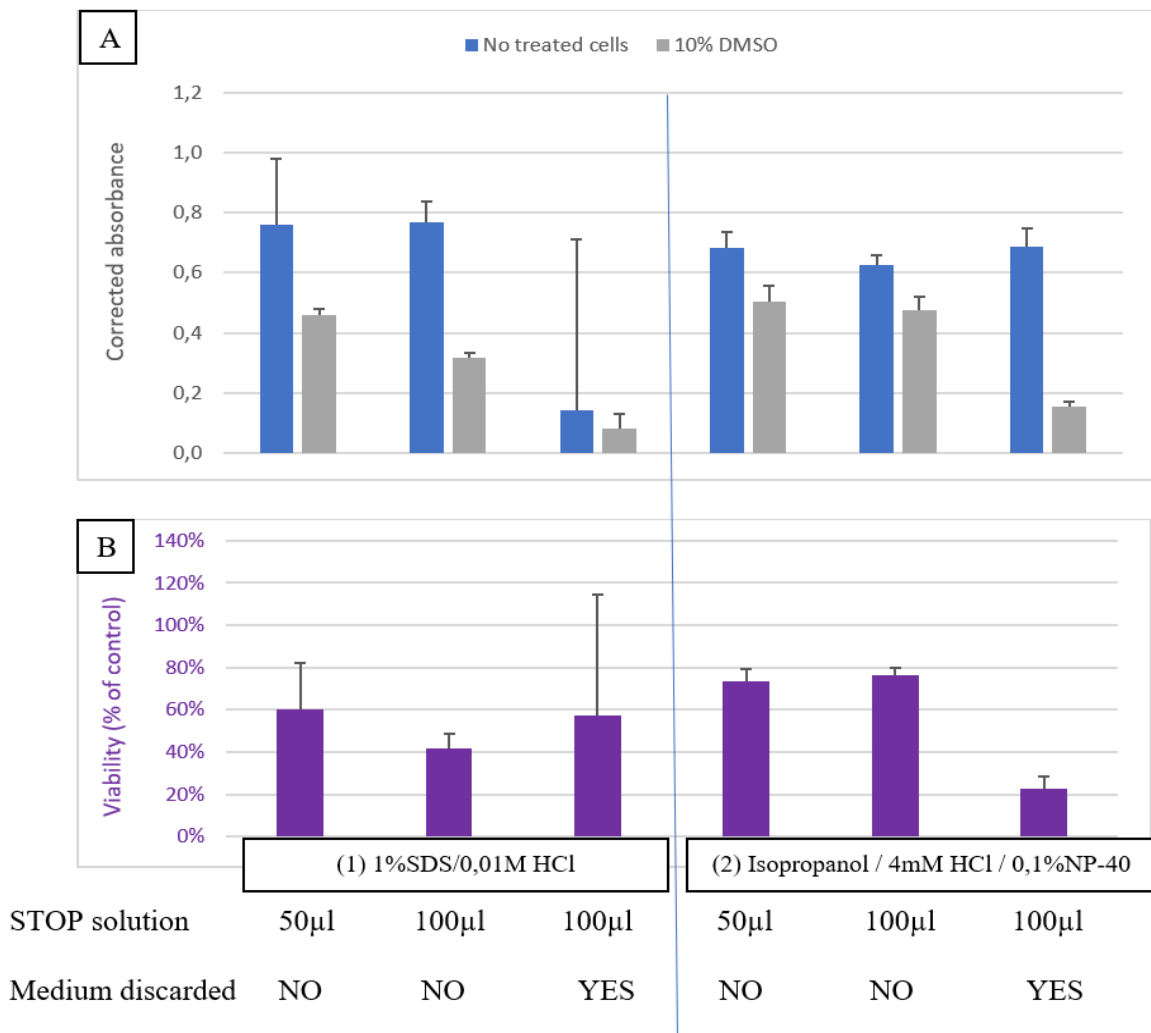
Figure 15: Corrected absorbance (560 nm -690 nm) (A) and calculated % of viability (B) resulting from dissolving formazan product of HepG2 cells seeded 24h in advance at 20 000 cells/well. Cells were treated or not with 10 % DMSO 4h before the MTT assay. After 1h incubation of cells with 10 µL MTT in solution at 5 mg/mL in PBS, formazan products were dissolved in stop solution (1) 1%SDS/0,01MHCl or (2) Isopropanol/4mMHCL/0,1%NP-40 without or with elimination of the medium. Each histogram shows the mean and standard deviation of 6 replicates (n=6).

In Figure 14 (A), it appears that the stop solution (2) (Isopropanol/4mMHCl/0,1%NP-40) showed the lowest overall variability (represented on the graph by vertical bar). In practice, it was difficult to avoid foam with the stop solution (1) containing 1%SDS/0,01MHCl, and these bubbles might interfere with the absorbance. Moreover, the results showed that discarding the

medium before adding the stop solution 2 helped detect a strong difference between non-treated (100 % viable) and 10 % DMSO treated cells (decrease of viability).

Therefore, condition with elimination of the medium and addition of 100 µL of the stop solution (2) (Isopropanol/4mMHCl/0,1%NP-40) was chosen for all the coming experiments.

3.1.1.2   MTT concentration and incubation time

MTT must be added at a certain concentration and to a certain time to be efficiently converted to formazan crystals. These parameters were tested on HepG2 seeded between 2500 to 20 000 cells (Figure 16).
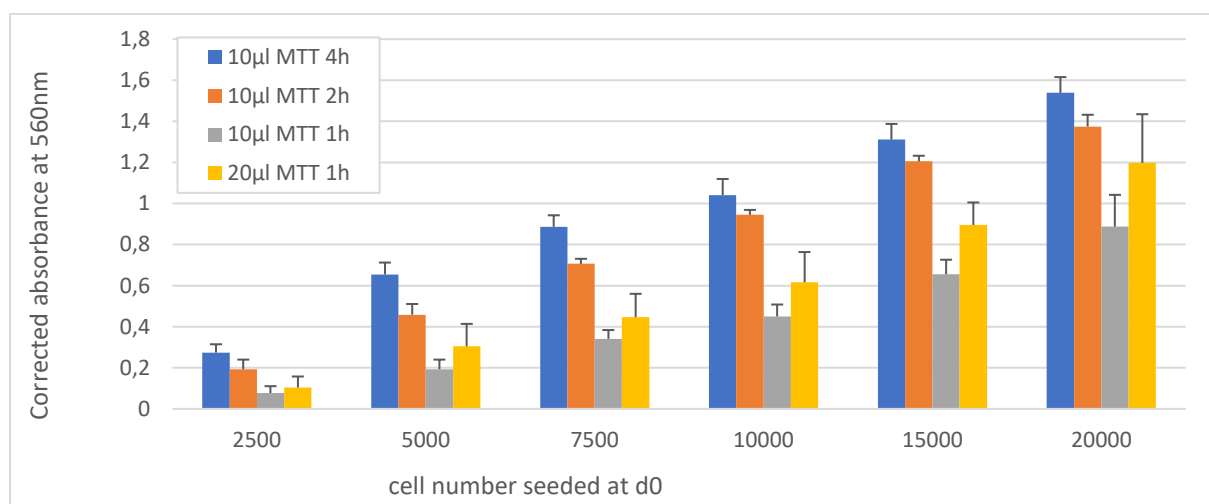
Figure 16: Comparison of the absorbances obtained after adding 10 µL or 20 µL of MTT at 5 mg/mL and an incubation time from 1h to 4h on an increased cell number of HepG2 seeded 2h in advance. Each histogram shows the mean and standard deviation of 6 replicates (n=6).

As expected, adding 2 times more of the MTT solution increases the absorbance (condition 1h plus 20 µL MTT vs 1h plus 10 µL MTT). However, the variability represented by the error bar are higher.

On the other hand, 4h incubation with MTT gave a higher absorbance, but it didn't improve as much as a 2h incubation time. Moreover, both MTT and the formazan product are toxic to cells therefore a long incubation with MTT itself may cause cell death. 2h incubation time being also the more convenient way to proceed, we chose to perform the MTT assay with 10 µL MTT at 5 mg/mL and a 2h incubation at 37°C.

3.1.1.3 10 000 cells per well is the optimal cell number

Linearity between cell number and absorbance

As the number of viable cells and absorbance are so reliant on each other, it is vital to optimize the cell number in each well to ensure that the measured absorbance is within a linear range. This optimization was performed by seeding different cell lines with a cell number evenly distributed from 2000 cells/well to 20 000 cells/well.

The correlation between cell number and the absorbance was performed one time at d0, to exclude the cell growth factor variable (Figure 17).
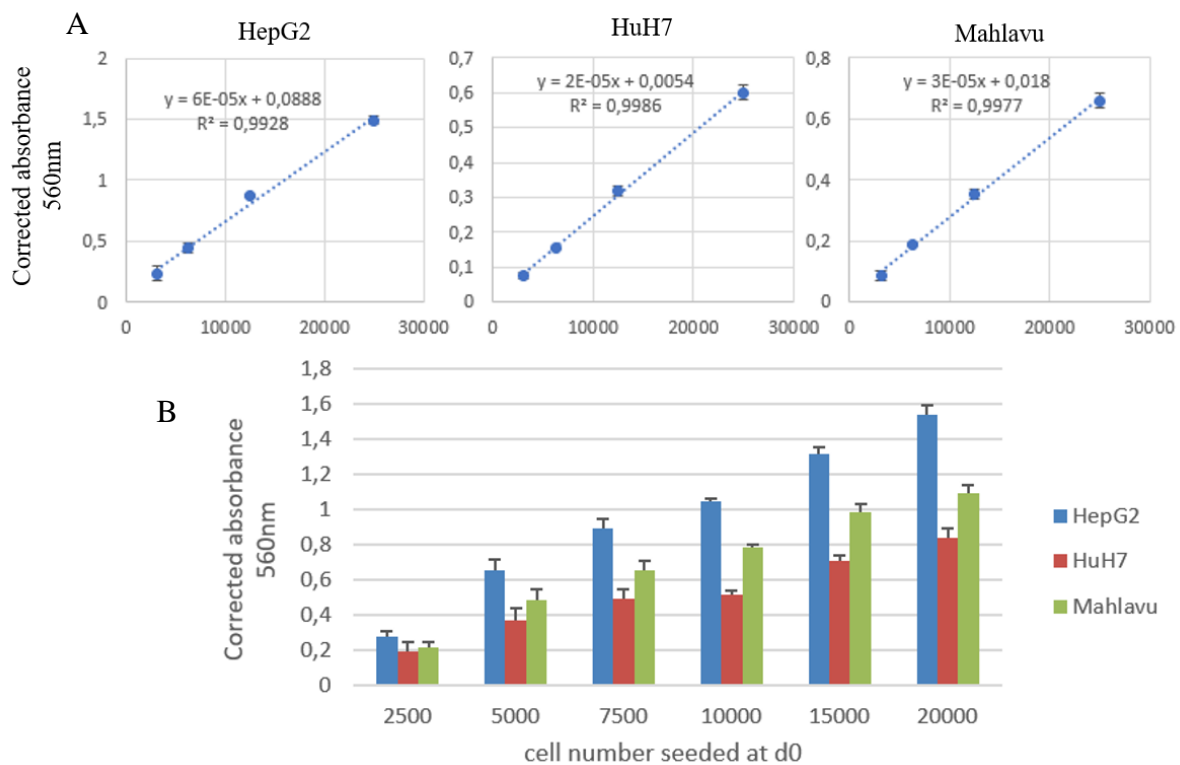
Figure 17: (A) Correlation between corrected absorbance and cell number in MTT assay in 3 different cell lines: HepG2, HuH7 and Mahlavu. The dashed line represents the linear least squares fit for the data; equation and the coefficient of determination R^2 are noted on each graph.

(B) Comparison of the absorbances in MTT assay between the 3 different cell lines at different cell concentrations. Each value is the mean of 6 replicates (n=6). The standard deviations are represented by vertical bars.

As shown in Figure 17, the repeatability of the assay was confirmed, and as expected, a nice correlation was observed between cell number and absorbance for all cell lines, with a R^2 calculated close to 1.

But the formazan produced is not only dependant on cell number as it is a test based on cell metabolism; it is also dependant of the cell type. In figure 17B, it is clearly demonstrated that HepG2 with the same number of cells as HuH7 and Mahlavu, has a higher rate of conversion. However, to compare the effect of AFB1, all values will be normalized on the non-treated control as the 100 % cell viability, resulting in comparable data.

10 000 cells per well is the optimal cell number to seed per well of a 96 well plate

The same experiment was performed 72h after the cells were plated to take into consideration the differences in cell growth in our different cell lines.
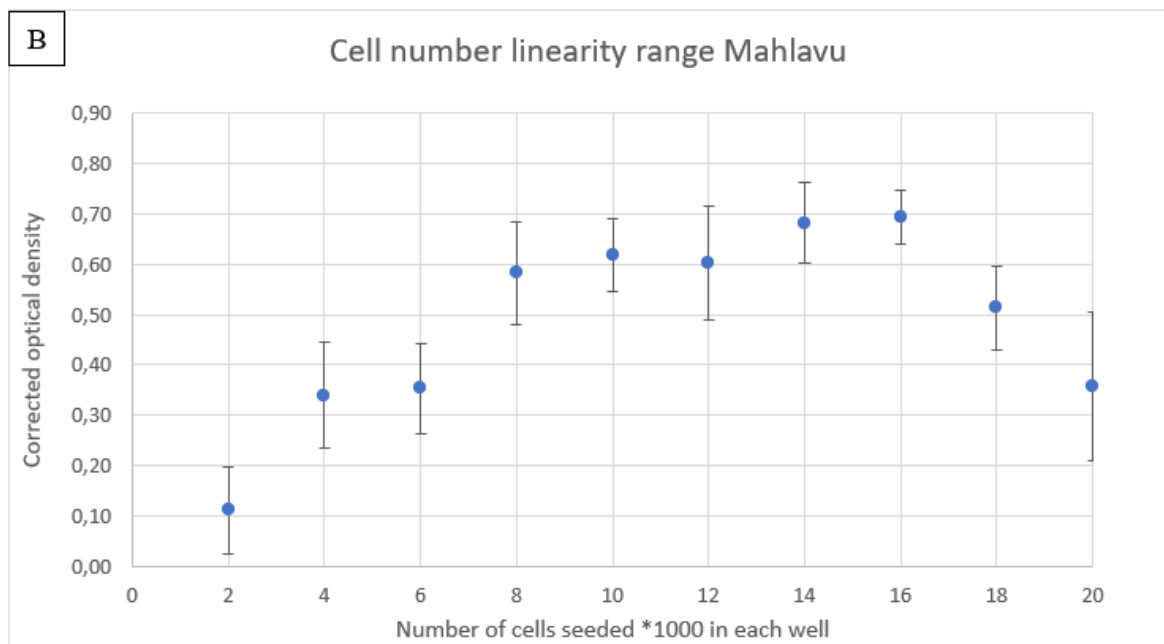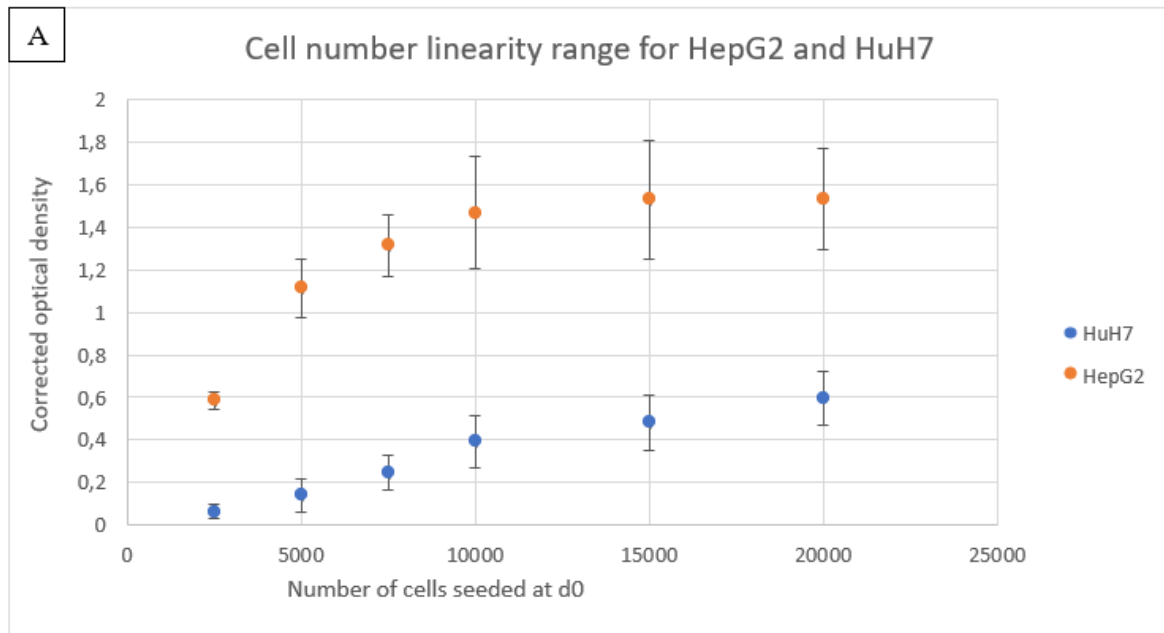
Figure 18: Correlation between cell number seeded and absorbance of the MTT assay for HepG2 and HuH7 (A) and Mahlavu (B). An evenly distributed number of cells in the range 2500 cells to 20 000 cells were seeded and the assay was performed 72h after seeding. Each value is the mean of 6 replicates (n=6). Standard deviation is represented by vertical bars.

The results in Figure 18 show that the cell lines reach a plateau at 10 000 cells/well, thus proving that the linear range of cell number for the MTT assay is 2000 to 10 000 cells/well. A good growth for the cells requires them to be in proximity to each other and not be too diluted, making 10 000 cells/well the optimal cell number for the MTT assay.

### 3.1.1.4 Treatment should not exceed 100 µM AFB1

The last focus of our optimizing of the MTT assay was the treatment with AFB1, as the assay was performed to detect its cytotoxic abilities. Our main concern was the fact that AFB1 had to be reconstituted in DMSO and the highest concentration possible was 30 mM. DMSO is known to be cytotoxic by itself, therefore an experiment with a high concentration of DMSO would not be relevant. A test to compare cell viability between non-treated cells and cells treated with either 250 µM AFB1 or the corresponding DMSO concentration (0,83 %) was performed (Table 3).

The % cell viability for the control (DMSO), as shown in Table 3, were quite low and in some instances, even lower than in the concentration of AFB1. This suggest that the diluent of AFB1 also has cytotoxic effects and has too much of an impact to know if the % cell viability of 250 µM AFB1 is due to the aflatoxin or the diluent.

Table 3: The difference in % cell viability between 250 µM AFB1 and DMSO 0,83 %. The table show the different cell lines with different length of treatment with AFB1 250 µM and DMSO 0,83 %. The % cell viability for DMSO is in some instances lower than for the aflatoxin.

| Cell line – interval	250 µM AFB1	DMSO 0,83 %
HepG2 – 24h	25,25 %	56,52 %
HuH7 – 24h	36,05 %	17,34 %
Mahlavu – 24h	29,32 %	60,21 %
HepG2 – 48h	25,32 %	54,24 %
HuH7 – 48h	14,52 %	72,27 %
Mahlavu – 48h	19,14 %	73,75 %
HepG2 – 72	57,56 %	45,12 %
HuH7 – 72h	24,12 %	37,44 %
Mahlavu – 72h	18,24 %	60,30 %

At 0,332 % DMSO, corresponding with the level of DMSO when cells are treated with 100 µM of AFB1, no significant difference were observed (Figure 18). Therefore, for our experiment comparison was made with cells treated with 0,332 % DMSO as the 100 % viable cells.
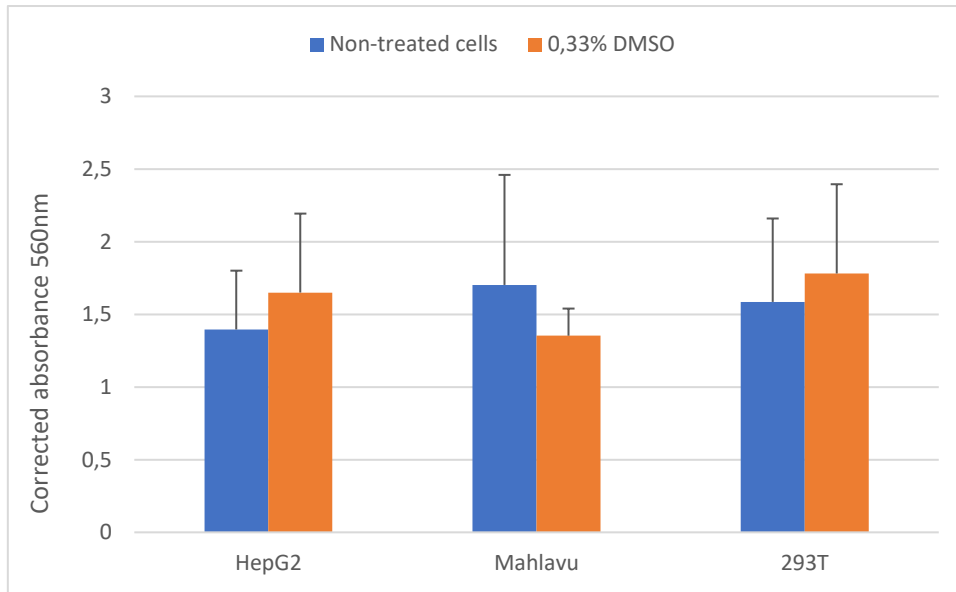
Figure 18: No significant difference was observed between cells treated with 0,332 % DMSO and non-treated cells for HepG2, Mahlavu and 293T. Each value is the average, and the variability is represented by vertical bars.

3.1.2   Cytotoxic effect of AFB1 treatment

After optimizing the MTT assay HuH7, HepG2 and Mahlavu were treated with AFB1 with concentrations in the range from 0,01 µM to 100 µM with 10 000 cells seeded in each well with a 24h, 48h and 72h treatment.
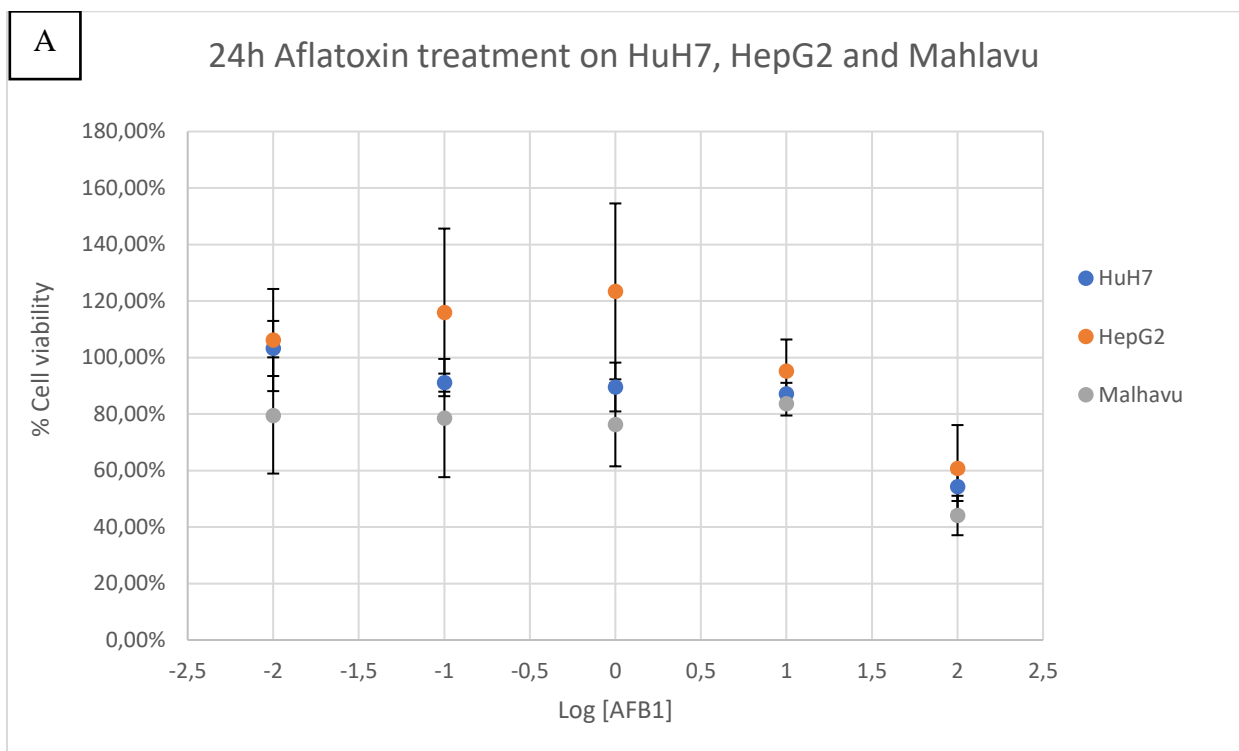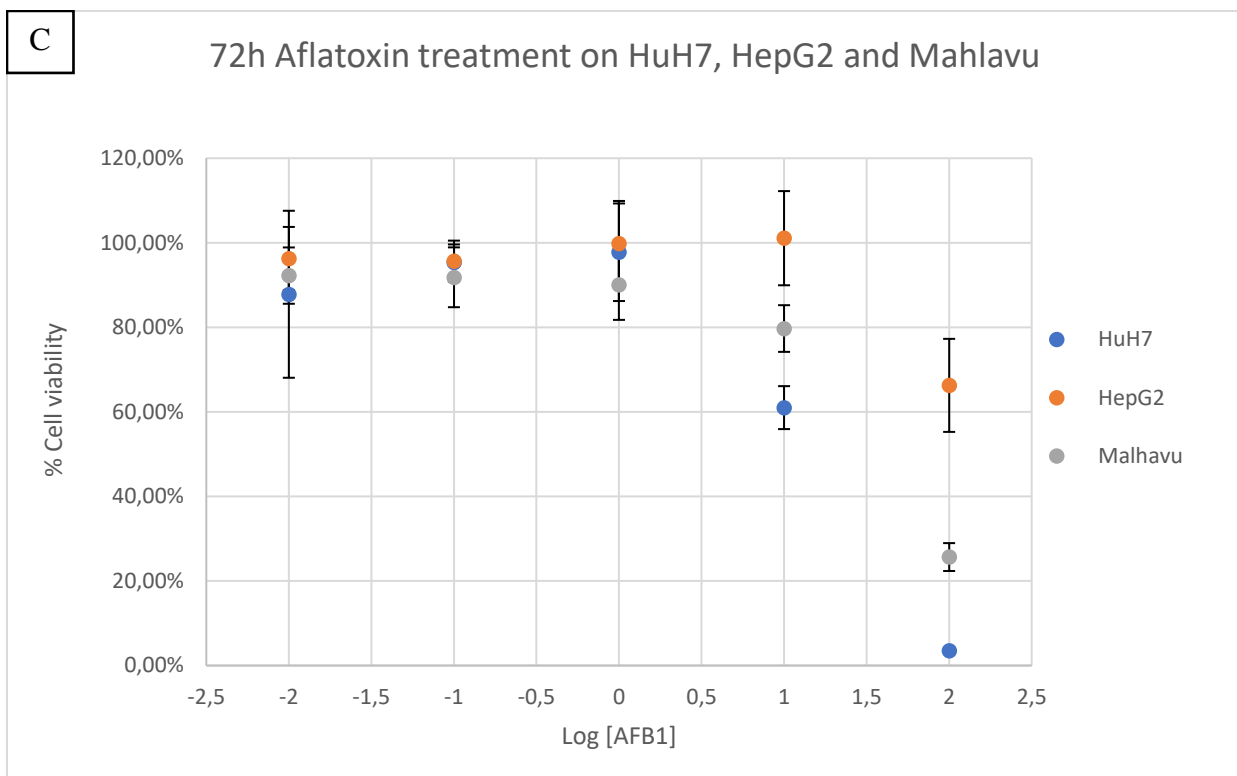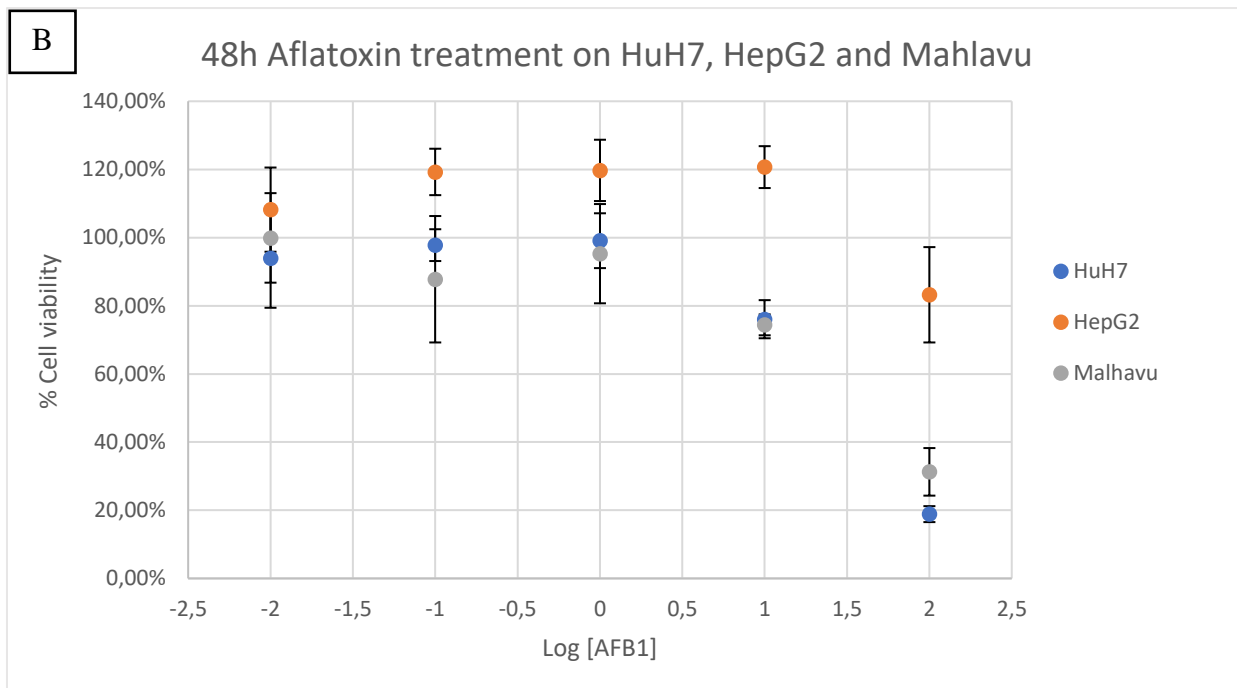
Figure 19: A 24h (A), 48h (B) and 72h (C) aflatoxin treatment on HuH7, HepG2 and Mahlavu show the cytotoxic effect of AFB1 on % cell viability. *The cell lines were seeded with 10 000 cells/well and treated with aflatoxin with concentrations 0,01 µM to 100 µM. After the treatment period (24h, 48h, 72h) the cells were added 10 µL MTT at 5 mg/mL and incubated for 2h. The wells were added 100 µL stop solution (Isopropanol/4mMHCl/0,1%NP-40) before reading at microplate reader. Each value is the mean of 3 to 4 replicates (n=3-4). The standard deviations are represented by vertical bars.*

The results show that HepG2 has a higher tolerance for AFB1 than HuH7 and Mahlavu (Figure 19).

Further, the comparison of calculated ED25% (Table 4) on 4 different experiments performed independently show that HepG2 indeed has a high tolerance for AFB1 while HuH7 is very sensitive, as it only requires 2,93 µM AFB1 to have 25 % of its cell line killed within 72h. However, this value is highly variable from one experiment to the other and should be taken with caution.

Table 4: HuH7 has a higher sensitivity to AFB1 concentrations and require thus only a small concentration to have 25 % of its colony dead. ED25% for HepG2, HuH7 and Mahlavu following a 24h, 48h or 72h treatment with average value and standard deviation.

Cell line	ED25% 24h treatment (µM)	ED25% 48h treatment (µM)	ED25% 72h treatment (µM)
HepG2	40,08 ± 42,033	36,51 ± 34,210	22,53 ± 15,726
HuH7	10,49 ± 9,405	10,03 ± 0,245	2,22 ± 0,998
Mahlavu	10,69 ± NaN	14,58 ± 6,923	10,29 ± 1,594

3.2 Long-term treatment assay results

3.2.1 Cell observable phenotype during the treatment

Our second objective in this project is to investigate if the induction of the R249S mutation on the *TP53* gene is an effect of a long-term exposure to AFB1. To mimic a chronic exposure, the cell lines HepG2 and HuH7 were exposed to the aflatoxin using a long-term treatment assay.

Comments on morphology and confluency as well as calculated cell concentration for each passage was noted (Tables 5, 6). This shows a higher sensitivity to AFB1 for HuH7 than HepG2.

Table 5: Comments and calculations from the LTA#1 for HepG2. The one Petri dish of the cell line was treated with 1 μM AFB1 and the other Petri dish was treated with the same volume of 33 % DMSO. The Petri dishes were seeded with 1*10^6 cells and the one with control was quickly lost due to evaporation of medium under incubation.

	Cell observations and comments		Cell count in Petri dish		% cell death	
	0 μM	1 μM	0 μM	1 μM	0 μM	1 μM
3 days of treatment	Confluency: 95 % Morphology: OK	Confluency: 95 % Morphology: OK	28,1*10^6 cells (6 mL)	32,2*10^6 cells (6 mL)	8,6 %	5,3 %
7 days of treatment	Confluency: 40 % Morphology: OK. Does not grow well	Confluency: 40 % Morphology: OK. Does not grow well	2,8*10^6 cells (3 mL)	1,6*10^6 cells (3 mL)	2,1 %	2,5 %
10 days of treatment	Confluency: 85 % Morphology: OK	Confluency: 85 % Morphology: OK	2,1*10^6 cells (5 mL)	5,9*10^6 cells (5 mL)	4,5 %	3,8 %
14 days of treatment	Confluency: 60 % Morphology: OK	Confluency: 50 % Morphology: OK	0,6*10^6 cells (3 mL)	1,2*10^6 cells (3 mL)	3,2 %	9,1 %
17 days of treatment	Cells died due to evaporation of medium	Confluency: 95 % Morphology: OK		6,1*10^6 cells (10 mL)		4,2 %
21 days of treatment		Confluency: 50 % Morphology: grows abnormally, very individualized		0,7*10^6 cells (5 mL)		25,0 %

24 days of treatment		Confluency: 30 % Morphology: not OK		1,0*10^6 cells (2 mL)		19,8 %
	Stopping LTA#1 for HepG2 because there are too few viable cells left and the control is already stopped.					

Table 6: Comments and calculations from the LTA#1 for HuH7. *One Petri dish of the cell line was treated with 1 µM AFB1 and the other Petri dish was treated with the same volume of 33 % DMSO. The Petri dishes were seeded with $1*10^6$ cells. This LTA was quickly stopped as HuH7 has a high sensitivity to AFB1, and the cells treated with the aflatoxin died too fast.*

	Cell observations and comments		Cell count in Petri dish		% cell death	
	0 µM	1 µM	0 µM	1 µM	0 µM	1 µM
3 days of treatment	Confluency: 100 % Morphology: OK	Confluency: 100 % Morphology: OK	$21,5*10^6$ cells (6 mL)	$11,4*10^6$ cells (6 mL)	3,2 %	5,0 %
7 days of treatment	Confluency: 55 % Morphology: OK	Confluency: 45 % Morphology: OK	$1,1*10^6$ cells (3 mL)	$0,2*10^6$ cells (3 mL)	0,0 %	2,7 %
10 days of treatment	Confluency: 90 % Morphology: OK	Confluency: 30 % Morphology: not OK. Many floating cells	$4,7*10^6$ cells (5 mL)	$0,1*10^6$ cells (5 mL)	0,8 %	33,3 %
14 days of treatment	Confluency: 65 % Morphology: OK	Only dead cells	Stopping LTA#1 for HuH7 because there are no viable cells left with the AFB1.			

Due to encountered problems with the LTA#1 such as evaporation of medium and passages dying too soon because of sensitivity, the assay had to be stopped sooner than expected and a new and improved LTA took place. However, these firsts results clearly showed that HuH7 were extremely sensitive to a low level AFB1 treatment on a long-term with a significant decrease in cell growth over time and an increase of cell death counted via Trypan blue staining.

The LTA#2 was performed on HepG2 and HuH7 (Tables 7, 8) and had several improvements. The second assay was more standardized to have more uniform data on each passage for each cell line, and there were taken photos each time to track the morphologic changes (Appendix

Tables 1, 2). The number of cells seeded was changed as HuH7 was more sensitive than expected, HepG2 continued with $1*10^6$ cells while HuH7 were seeded with $2*10^6$ cells. 0,1 µM AFB1 treatment was also added to keep our cells growing for a longer time.

Table 7: Comments and calculations from the LTA#2 for HepG2. The Petri dishes were seeded with $1*10^6$ cells and treated with 0,1 and 1 µM AFB1.

	Cell observations and comments		Cell count in Petri dish		% cell death	
	0,1 µM	1 µM	0,1 µM	1 µM	0,1 µM	1 µM
4 days of treatment	Confluency: 80 % Morphology: OK	Confluency: 70 % Morphology: OK	$4,4*10^6$ cells (5 mL)	$2,6*10^6$ cells (5 mL)	14,3 %	9,3 %
7 days of treatment	Confluency: 45 % Morphology: OK	Confluency: 70 % Morphology: OK	$2,3*10^6$ cells (5 mL)	$4,7*10^6$ cells (5 mL)	7,9 %	11,8 %
11 days of treatment	Confluency: 40 % Morphology: OK	Confluency: 55 % Morphology: OK	$4,7*10^6$ cells (5 mL)	$6,8*10^6$ cells (5 mL)	4,7 %	2,9 %
14 days of treatment	Confluency: 70 % Morphology: OK	Confluency: 60 % Morphology: OK	$5,9*10^6$ cells (5 mL)	$4,9*10^6$ cells (5 mL)	5,3 %	6,6 %
17 days of treatment	Confluency: 90 % Morphology: OK	Confluency: 80 % Morphology: OK	$12,9*10^6$ cells (10 mL)	$12,1*10^6$ cells (10 mL)	7,2 %	8,1 %
20 days of treatment	Confluency: 80 % Morphology: OK	Confluency: 60 % Morphology: OK	$6,5*10^6$ cells (10 mL)	$4,1*10^6$ cells (10 mL)	5,8 %	14,1 %
24 days of treatment	Confluency: 90 % Morphology: OK	Confluency: 90 % Morphology: OK				
Stopping LTA#2 for HepG2						

Table 8: Comments and calculations from the LTA#2 for HuH7. The Petri dishes were seeded with $2*10^6$ cells and treated with 0,1 and 1 µM AFB1. The passage with 1 µM AFB1 had to be stopped soon as the cells did not look good and were about to die. These were pelleted for further analysis.

|	Cell observations and comments		Cell count in Petri dish		% cell death	
	0,1 µM	1 µM	0,1 µM	1 µM	0,1 µM	1 µM
4 days of treatment	Confluency: 95 % Morphology: OK	Confluency: 70 % Morphology: OK	$4,7*10^6$ cells (5 mL)	$5,9*10^6$ cells (5 mL)	14,1 %	3,8 %
7 days of treatment	Confluency: 85 % Morphology: OK	Confluency: 60 % Morphology: OK	$6,6*10^6$ cells (5 mL)	$3,2*10^6$ cells (5 mL)	0,5 %	1,0 %
11 days of treatment	Confluency: 60 % Morphology: OK	Confluency: 10 % Morphology: not OK. Cells are not attached to each other, lots of floating cells	$6,5*10^6$ cells (5 mL)	$0,9*10^6$ cells (5 mL)	4,0 %	12,5 %
14 days of treatment	Confluency: 85 % Morphology: OK	Confluency: 50 % Morphology: not OK. Very big cells and individualized, lots of floating cells	$3,8*10^6$ cells (10 mL)	$1,1*10^6$ cells (3 mL)	6,6 %	15,9 %
17 days of treatment	Confluency: 90 % Morphology: OK	STOP	$10,2*10^6$ cells (10 mL)		11,0 %	
20 days of treatment	Confluency: 60 % Morphology: OK		$3,8*10^6$ cells (10 mL)		3,4 %	
24 days of treatment	Confluency: 65 % Morphology: OK					
	Stopping LTA#2 for HuH7					

3.2.2 Detection of the R249S mutation

First RFLP was performed on the non-treated cells. Mahlavu gDNA extract was used as a positive control of mutated sample (Figure 20). This PCR validates that Mahlavu really is a mutated cell line, as it only has bands at 158bp as the little shift from undigested to digested mutated band is visible. The result for HepG2, HuH7 and Hep3B however is not as conclusive. They all have the expected bands at 92bp and 66bp, but they all have a faint band at the mutated band size. This contamination requires a new PCR to give conclusive results.
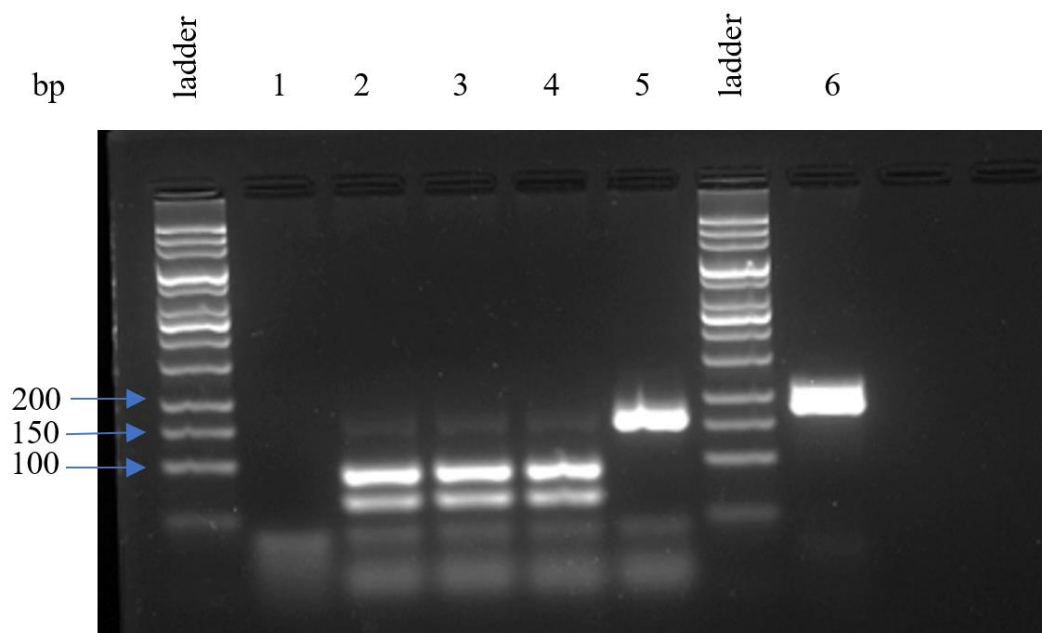
Figure 20: Validation of Mahlavu cell line. This PCR result validates that Mahlavu indeed is the mutated cell line with a strong band at 158bp. The samples in respective order from the left: ladder, H₂O (1), HepG2 (2), HuH7 (3), Hep3B (4), Mahlavu (5), ladder, undigested Mahlavu (6). Contamination in cell lines HepG2, HuH7 and Hep3B leaves the result inconclusive at this point.

As the results from the first PCR leaves the mutation status for HepG2, HuH7 and Hep3B non-conclusive, a new PCR was performed with only HepG2 samples to avoid contamination coming from the Malhavu sample as shown in Figure 21. This too has contamination with DNA fragments at 158bp, the band length of the mutated fragment.
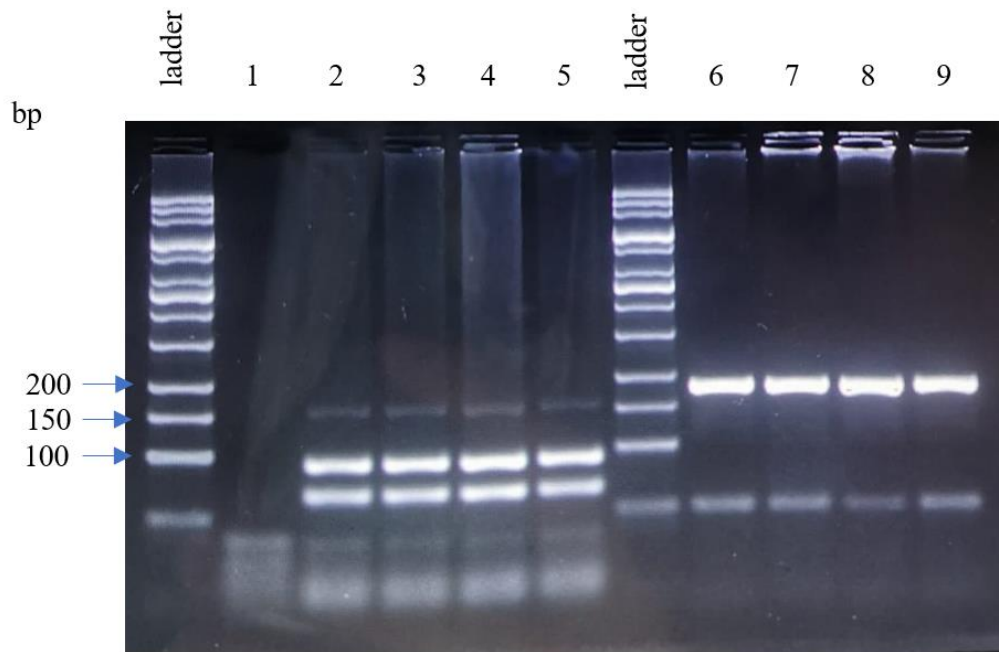
Figure 21: Still contamination in the PCR for HepG2, HuH7 and Hep3B. *The samples in respective order from the left: ladder, H$_2$O (1), HepG2 (2), HepG2 (3), HuH7 (4), Hep3B (5), ladder, undigested HepG2 (6), undigested HepG2 (7), undigested HuH7 (8), undigested Hep3B (9). The mutation status result on hotspot R249S on TP53 gene remain inconclusive.*

Nucleic acid amplification tests are very sensitive methods, and as a consequence, risks of contamination are high. Currently, no PCR on the gDNA extracted from the LTA#1 and #2 was performed as we would not be able to conclude: would the faint band corresponding at the mutated fragment be real or would it be a contamination?

New primers and reagents were ordered to repeat the RFLP with minimum risk of contamination.

4   Discussion

This internship was performed in a newly established research lab at UCLy, meaning that development of procedures and protocols required more of the available time than we had anticipated. This was partly due to problems related to evaporation which led to the loss of certain cell lines, cell lines being more demanding and required a longer period to obtain a regular growth rate and contamination in our PCR results. Due to these problems, the time available for optimizing the MTT and generate cell viability data was drastically shortened and made the period too short to experiment on all our cell lines.

4.1   Limitation of the MTT assay

The MTT assay was chosen as a first method to assess the cell survival of our different cell lines during an AFB1 treatment.

It was clear that we needed to optimize different parameters and to check our experimental conditions for each cell line.

By using preliminary experiments with different stop solutions, different cell numbers and different AFB1 concentrations, the final protocol for our laboratory ended with 100 µL Isopropanol/4mMHCl/0,1%NP-40 with discarding the medium as the stop solution, 10 000 cells seeded per well and treatment with AFB1 in the range 0,01 µM to 100 µM AFB1. The upper limit of aflatoxin was determined due to the cytotoxic influence from DMSO at higher concentrations of AFB1, as the aflatoxin is reconstituted in DMSO as solvent.

These optimizations are of course time consuming but crucial to be able to generate significant and reproducible results.

However, it is clear that MTT assay, considered as a golden standard, is not the most sensitive way to determine cell viability. This is also shown by the big variations between the duplicates for the calculated ED25%. Therefore, the team also plan to set up other assays like CellTiter-Glo® Luminescent Cell Viability Assay based on quantification of the ATP present as an indicator of metabolically active cells, via the detection of a sensitive luminescent signal. Both methods will be compared in term of sensitivity and reproducibility.

4.2 No advantages were given by the R249S mutation in our cell line models after AFB1 exposure

MTT results from AFB1 treatments were generated after the MTT assay was optimized. The results showed the % cell viability for HepG2, HuH7 and Mahlavu following 24h, 48h and 72h treatment with a range of concentrations of AFB1 from 0,01 µM to 100 µM in 10 000 cells/well. These results show the difference in AFB1 sensitivity across the different cell lines with HepG2 (wild type) being the most tolerant and HuH7 (overexpression p53) being the most sensitive cell line. Mahlavu is also quite sensitive.

Therefore, based on the results the hypothesis that the R249S mutation would confer a resistance to an AFB1 exposure is not confirmed. The mutated cell line does not seem to favor cell survival or proliferation during an AFB1 treatment, nor does an overexpression of the p53. The cell line that has the highest tolerance is HepG2, the cell line possessing the p53 wild type. However, it is only preliminary results as this experiment must be repeated to confirm or not our conclusion.

Another unexpected result was the fact that we were unable to calculate the ED50% as the AFB1 treatment from 0,01 µM to 100 µM didn't induce the appropriate level of cell death. It is not consistent with other published data (Table 9).

Table 9: Calculated ED50% on HepG2 from different published articles.

Cell type	Treatment incubation	Concentrations AFB1	ED50%	Reference
HepG2	72h	0-100 µM	~15 µM	(Huang et al., 2017)
HepG2	48h		>75,9 µM	(Ishida et al., 2020)
HepG2		0-10 µM	2,5 µM	(Desaulniers et al., 2021)

One hypothesis is that our HepG2 cell line derived and lost their content in metabolic active CYP450 enzymes necessary for the conversion of the AFB1 to its genotoxic metabolite. However, our HepG2 showed a very high metabolic activity via more active conversion of MTT to formazan than HuH7 and Malhavu cells.

Different strategies will be used to understand why our HepG2 seem so resistant to an AFB1 treatment (Table 10).

Table 10: Hypothesises with corresponding perspectives to explain why HepG2 seems resistant to AFB1 treatment.

Hypothesis	Perspective
Derivation of our HepG2	Repeat the experiment on newly ordered HepG2 fully characterized and validated
AFB1 was not metabolized	Add Microsomes from Liver, Pooled from rat (Sprague-Dawley) (sigmaaldrich.com, M9066)
	Inhibit CYP450 using 1-Aminobenzotriazole (sigmaaldrich.com, 1614-12-6)

4.3 Long term treatment to induce the apparition of a R249S mutation

A chronic exposure to aflatoxin B1 was mimicked by performing a long-term treatment assay on two cell lines with different mutation status on p53.

The first LTA had to be stopped quite quickly due to different problems. As it was not standardized, the results gave suggestions to what should be improved, e.g., number of cells seeded for each cell line.

For HepG2, the wild type cell line, the LTA#1 had a decline in confluency and cell concentration for both the non-treated and the 1 µM AFB1 treated cells. The strongest hypothesis is that the decline was due to technical problems arising from the incubator in the cell culture room, emphasizing the fact that materials in the laboratory are important and pose as factors of variation.

The LTA#1 for HuH7, the cell line with a p53 overexpression, was only able to last two weeks due to the cell line's sensitivity to the aflatoxin. This is consistent with the results from the MTT assays.

The LTA#2 was an improved version, with changes to AFB1 concentrations and cell numbers in each Petri dish. The cell lines were treated with 0,1 µM and 1 µM AFB1 and were compared to a Petri dish of non-treated cells of the same cell line.

This time the HepG2 did well with both concentrations, even though the number of seeded cells stayed the same as LTA#1. Towards the end of the assay the confluency was stabilized over

80 %. The % cell death had no major deviances, with values scattered under 15 %. Cell concentrations were stable and OK until the last count.

The LTA#2 for HuH7 was adjusted to its sensitivity by seeding $2*10^6$ cells per Petri dish. While the Petri dish with 0,1 µM AFB1 treated cells did well and maintained a good confluency and morphology, the 1 µM treated did not. The confluency declined drastically after three passages and showed abnormal growth and morphology. At the last passage the treated cells were abnormally big, up to 100x the size of a normal cell. This proves that this cell line is very sensitive to the aflatoxin, even at small concentrations (1 µM AFB1).

Since this experiment was performed on a wild type cell line and a cell line with overexpression of p53, it would not be complete without doing a PCR to conclude if the cell lines really have induced the R249S mutation. However, due to contamination of unknown source in the PCR reactions, this was not currently possible.

In conclusion, our question whether a long-term exposure to AFB1 induces the R249S mutation remains for the moments unconclusive. The lack of PCR results and that the period for the project did not allow to finish a 45 day long-term treatment assay, leaves us with no real data. The experiment did however depict the high sensitivity HuH7 has to the aflatoxin, which is corresponding to the findings from the MTT assay.

5   Conclusion

Our hypothesis that the R249S mutation on *TP53* gene would favor cell survival during an AFB1 treatment wasn't demonstrated using our different cell lines as models. The absence of the R249S mutation will favor cell survival during a treatment, while the cell lines with overexpression and mutated p53 will favor apoptosis. Both the MTT assay and the LTA show that HuH7 has a high sensitivity to even small concentrations of AFB1.

6 Perspectives

An understanding of the mechanisms responsible for the increase in the HCC in patients exposed to AFB1 is still under investigation and as a perspective, this first study on AFB1 exposure will be in the future coupled with study on the mechanisms on the synergic effect between a chronical HBV infection and AFB1.

Our objectives will be further investigated as this is a complex picture and a field in science that needs more research. As for now, there is no direct evidence behind the correlations between HCC incidence, AFB1 exposure and the frequency of the R249S mutation on *Tp53* gene. Obtaining evidence either supporting or weakening the correlation will give a better understanding and will hopefully lead to more research to the benefits of the patients. HCC takes many lives every year, and more research on this specific mutation and creation of sensitive detection methods could lead to earlier diagnosis and better prognosis.

For future experiments of this kind, the MTT assays should be performed on all the liver cancer cell lines multiple times to obtain significant reproductible results. Other cell viability assays must be also performed.

In order to get a more physiological cell model, the use of 3D spheroid culture mimicking tumoral cell organization in the organism, will be a model to obtain more clues as to how the mutated cells impact each other *in vivo*.

The LTA should be performed for 45 days or longer, and on multiple cell lines. The apparition of the mutation should then be validated by the use of RFLP technique with great care to do not introduce contamination.

7   References

293T | ATCC. (n.d.). Retrieved May 26, 2022, from https://www.atcc.org/products/crl-3216

Aden, D. P., Fogel, A., Plotkin, S., Damjanov, I., & Knowles, B. B. (1979). Controlled synthesis
of HBsAg in a differentiated human liver carcinoma-derived cell line. *Nature*,
282(5739), 615–616. https://doi.org/10.1038/282615a0

Alberts, B., Hopkin, K., Johnson, A., Morgan, D., Raff, M., Roberts, K., & Walter, P. (2019).
Essential cell biology (Fifth edition.; International student edition.). W. W. Norton &
Company.

Alshannaq, A. F., Gibbons, J. G., Lee, M.-K., Han, K.-H., Hong, S.-B., & Yu, J.-H. (2018).
Controlling aflatoxin contamination and propagation of Aspergillus flavus by a soy-
fermenting Aspergillus oryzae strain. *Scientific Reports*, *8*(1), 16871.
https://doi.org/10.1038/s41598-018-35246-1

Amaike, S., & Keller, N. P. (2011). Aspergillus flavus. *Annual Review of Phytopathology*, *49*,
107–133. https://doi.org/10.1146/annurev-phyto-072910-095221

Aspergillus flavus under microscope | Medical Laboratories. (n.d.). Retrieved May 27, 2022,
from http://www.medical-labs.net/aspergillus-flavus-under-microscope-1450/

Benkerroum, N. (2020). Chronic and Acute Toxicities of Aflatoxins: Mechanisms of Action.
International Journal of Environmental Research and Public Health, *17*(2), 423.
https://doi.org/10.3390/ijerph17020423

Bennett, J. W., & Klich, M. (2003). Mycotoxins. *Clinical Microbiology Reviews*, *16*(3), 497–
516. https://doi.org/10.1128/CMR.16.3.497-516.2003

BLAST. (n.d.). Retrieved April 20, 2022, from https://www.uniprot.org/uniprot/P04637

COSMIC | SBS - Mutational Signatures. (n.d.). Retrieved May 26, 2022, from
https://cancer.sanger.ac.uk/signatures/sbs/

Desaulniers, D., Cummings-Lorbetskie, C., Leingartner, K., Xiao, G.-H., Zhou, G., & Parfett, C.
(2021). Effects of vanadium (sodium metavanadate) and aflatoxin-B1 on cytochrome
p450 activities, DNA damage and DNA methylation in human liver cell lines.
Toxicology in Vitro, *70*, 105036. https://doi.org/10.1016/j.tiv.2020.105036

Fouad, A. M., Ruan, D., El-Senousey, H. K., Chen, W., Jiang, S., & Zheng, C. (2019). Harmful
Effects and Control Strategies of Aflatoxin B1 Produced by Aspergillus flavus and
Aspergillus parasiticus Strains on Poultry: Review. *Toxins*, *11*(3), 176.
https://doi.org/10.3390/toxins11030176

Genetic engineering and gene silencing could fight deadly crop mycotoxins—If not blocked

 by activists. (2017, October 18). *Genetic Literacy Project*.

 https://geneticliteracyproject.org/2017/10/18/genetic-engineering-gene-silencing-

 fight-scourge-crop-mycotoxins-food-not-blocked-activists/

Hep 3B2.1-7 [Hep 3B, Hep-3B, Hep3B] | ATCC. (n.d.). Retrieved May 26, 2022, from

 https://www.atcc.org/products/hb-8064

Hsu, I. C., Metcalf, R. A., Sun, T., Welsh, J. A., Wang, N. J., & Harris, C. C. (1991). Mutational

 hot spot in the p53 gene in human hepatocellular carcinomas. *Nature*, *350*(6317),

 427–428. https://doi.org/10.1038/350427a0

Huang, M. N., Yu, W., Teoh, W. W., Ardin, M., Jusakul, A., Ng, A. W. T., Boot, A., Abedi-

 Ardekani, B., Villar, S., Myint, S. S., Othman, R., Poon, S. L., Heguy, A., Olivier, M.,

 Hollstein, M., Tan, P., Teh, B. T., Sabapathy, K., Zavadil, J., & Rozen, S. G. (2017).

 Genome-scale mutational signatures of aflatoxin in cells, mice, and human tumors.

 Genome Research, *27*(9), 1475–1486. https://doi.org/10.1101/gr.220038.116

Hussain, S. P., Schwank, J., Staib, F., Wang, X. W., & Harris, C. C. (2007). TP53 mutations and

 hepatocellular carcinoma: Insights into the etiology and pathogenesis of liver cancer.

 Oncogene, *26*(15), 2166–2176. https://doi.org/10.1038/sj.onc.1210279

IARC. (n.d.). *Some Naturally Occurring Substances: Food Items and Constituents, Heterocyclic*

 Aromatic Amines and Mycotoxins. Retrieved May 28, 2022, from

 https://publications.iarc.fr/Book-And-Report-Series/Iarc-Monographs-On-The-

 Identification-Of-Carcinogenic-Hazards-To-Humans/Some-Naturally-Occurring-

 Substances-Food-Items-And-Constituents-Heterocyclic-Aromatic-Amines-And-

 Mycotoxins-1993

Ishida, Y., Yamasaki, C., Iwanari, H., Yamashita, H., Ogawa, Y., Yanagi, A., Furukawa, S.,

 Kojima, Y., Chayama, K., Kamiie, J., & Tateno, C. (2020). Detection of acute toxicity of

 aflatoxin B1 to human hepatocytes in vitro and in vivo using chimeric mice with

 humanized livers. *PloS One*, *15*(9), e0239540.

 https://doi.org/10.1371/journal.pone.0239540

Kastenhuber, E. R., & Lowe, S. W. (2017). Putting p53 in Context. *Cell*, *170*(6), 1062–1078.

 https://doi.org/10.1016/j.cell.2017.08.028

Kelly, J. D., Eaton, D. L., Guengerich, F. P., & Coulombe, R. A. (1997). Aflatoxin B1 activation in human lung. *Toxicology and Applied Pharmacology*, *144*(1), 88–95. https://doi.org/10.1006/taap.1997.8117

Kew, M. C. (2013). Aflatoxins as a cause of hepatocellular carcinoma. *Journal of Gastrointestinal and Liver Diseases: JGLD*, *22*(3), 305–310.

Lee, T. K.-W., Guan, X.-Y., & Ma, S. (2022). Cancer stem cells in hepatocellular carcinoma—From origin to clinical implications. *Nature Reviews Gastroenterology & Hepatology*, *19*(1), 26–44. https://doi.org/10.1038/s41575-021-00508-3

List of Classifications – IARC Monographs on the Identification of Carcinogenic Hazards to Humans. (n.d.). Retrieved May 28, 2022, from https://monographs.iarc.who.int/list-of-classifications

Liu, Y., & Wu, F. (2010). Global Burden of Aflatoxin-Induced Hepatocellular Carcinoma: A Risk Assessment. *Environmental Health Perspectives*, *118*(6), 818–824. https://doi.org/10.1289/ehp.0901388

Liver Cancer Cell Lines Database. (n.d.-a). Retrieved May 26, 2022, from https://lccl.zucmanlab.com/hcc/cellLines/Mahlavu

Liver Cancer Cell Lines Database. (n.d.-b). Retrieved June 6, 2022, from https://lccl.zucmanlab.com/hcc/cellLines/PLC.PRF5

Marchese, S., Polo, A., Ariano, A., Velotto, S., Costantini, S., & Severino, L. (2018). Aflatoxin B1 and M1: Biological Properties and Their Involvement in Cancer Development. *Toxins*, *10*(6), 214. https://doi.org/10.3390/toxins10060214

Menendez, D., Nguyen, T.-A., Resnick, M. A., & Anderson, C. W. (2018). P53. In S. Choi (Ed.), *Encyclopedia of Signaling Molecules* (pp. 3740–3755). Springer International Publishing. https://doi.org/10.1007/978-3-319-67199-4_57

Mosmann, T. (1983). Rapid colorimetric assay for cellular growth and survival: Application to proliferation and cytotoxicity assays. *Journal of Immunological Methods*, *65*(1), 55–63. https://doi.org/10.1016/0022-1759(83)90303-4

Nakabayashi, H., Taketa, K., Miyano, K., Yamane, T., & Sato, J. (1982). Growth of human hepatoma cells lines with differentiated functions in chemically defined medium. *Cancer Research*, *42*(9), 3858–3863.

Papachristou, F., Anninou, N., Koukoulis, G., Paraskakis, S., Sertaridou, E., Tsalikidis, C., Pitiakoudis, M., Simopoulos, C., & Tsaroucha, A. (2021). Differential effects of

cisplatin combined with the flavonoid apigenin on HepG2, Hep3B, and Huh7 liver cancer cell lines. *Mutation Research/Genetic Toxicology and Environmental Mutagenesis*, *866*, 503352. https://doi.org/10.1016/j.mrgentox.2021.503352

Perri, F., Pisconti, S., & Della Vittoria Scarpati, G. (2016). P53 mutations and cancer: A tight linkage. *Annals of Translational Medicine*, *4*(24), 522. https://doi.org/10.21037/atm.2016.12.40

Schwab, M. (Ed.). (2017). *Encyclopedia of Cancer*. Springer Berlin Heidelberg. https://doi.org/10.1007/978-3-662-46875-3

Tada, H., Shiho, O., Kuroshima, K., Koyama, M., & Tsukamoto, K. (1986). An improved colorimetric assay for interleukin 2. *Journal of Immunological Methods*, *93*(2), 157–165. https://doi.org/10.1016/0022-1759(86)90183-3

The Overview of Cell Viability. (n.d.). CUSABIO. Retrieved May 30, 2022, from https://www.cusabio.com/c-21030.html

Twentyman, P. R., & Luscombe, M. (1987). A study of some variables in a tetrazolium dye (MTT) based assay for cell growth and chemosensitivity. *British Journal of Cancer*, *56*(3), 279–285.

Wang, W., & Wei, C. (2020). Advances in the early diagnosis of hepatocellular carcinoma. *Genes & Diseases*, *7*(3), 308–319. https://doi.org/10.1016/j.gendis.2020.01.014

Zhou, X., Hao, Q., & Lu, H. (2019). Mutant p53 in cancer therapy—The barrier or the path. *Journal of Molecular Cell Biology*, *11*(4), 293–305. https://doi.org/10.1093/jmcb/mjy072
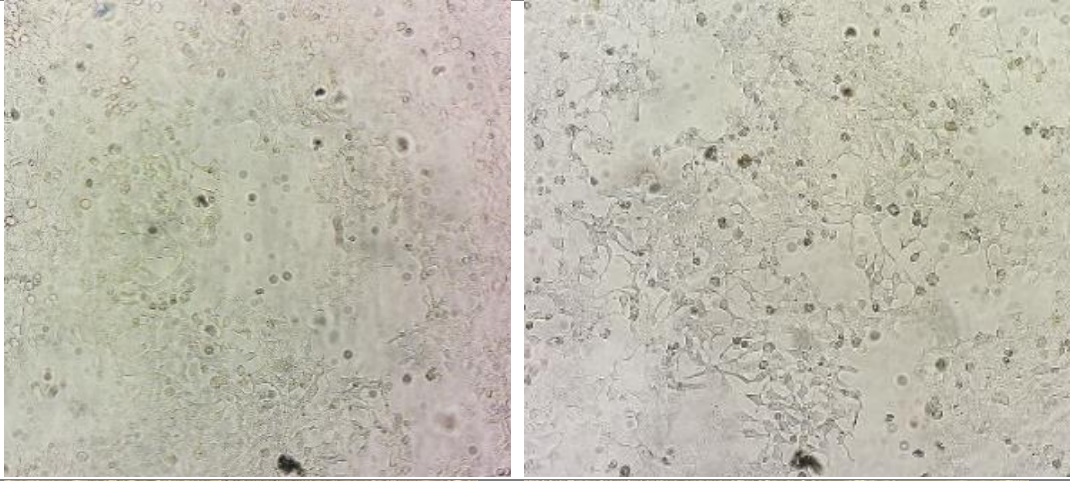
8   Appendix

8.1   LTA#2 HepG2 pictures

Appendix Table 1: Pictures from each passage done in the LTA#2 on HepG2. Each passage was seeded with $1*10^6$ cells.
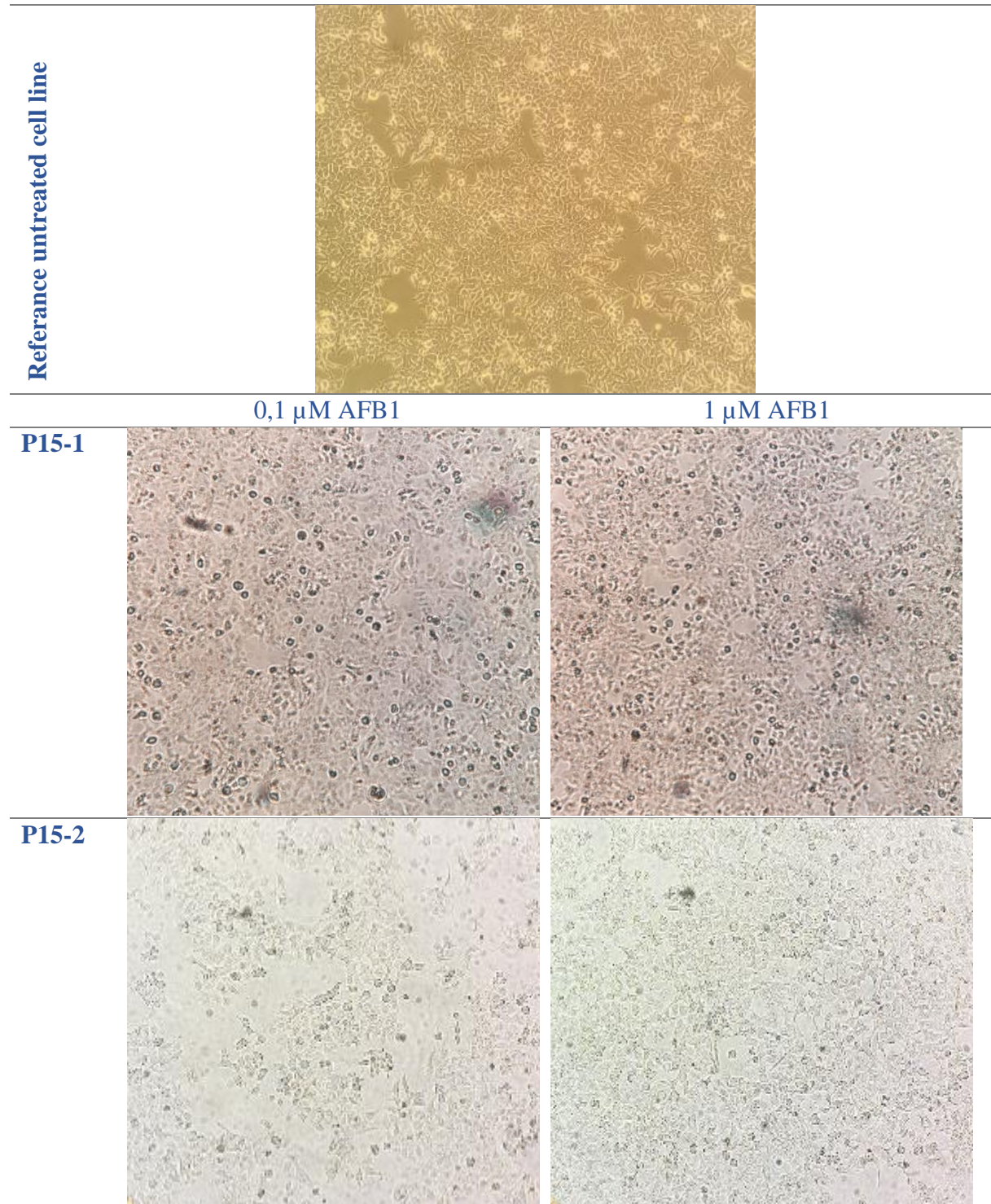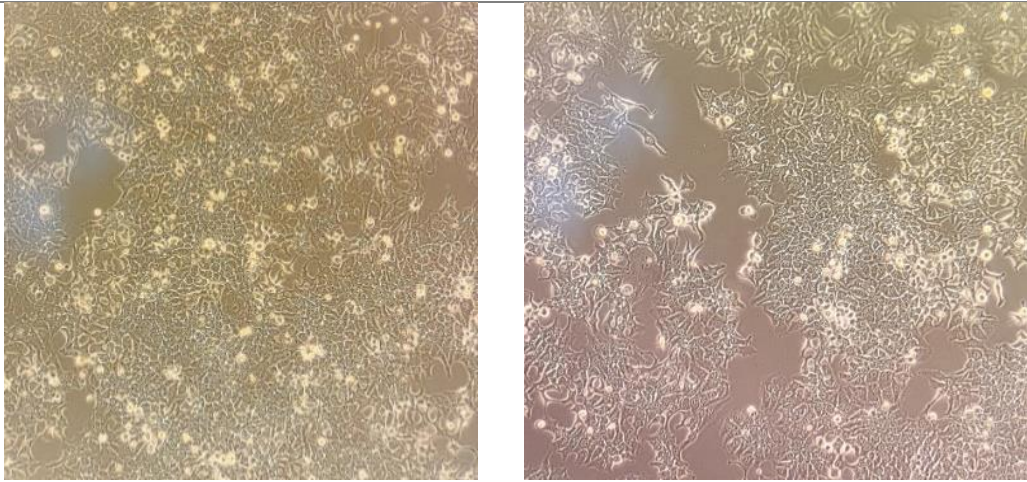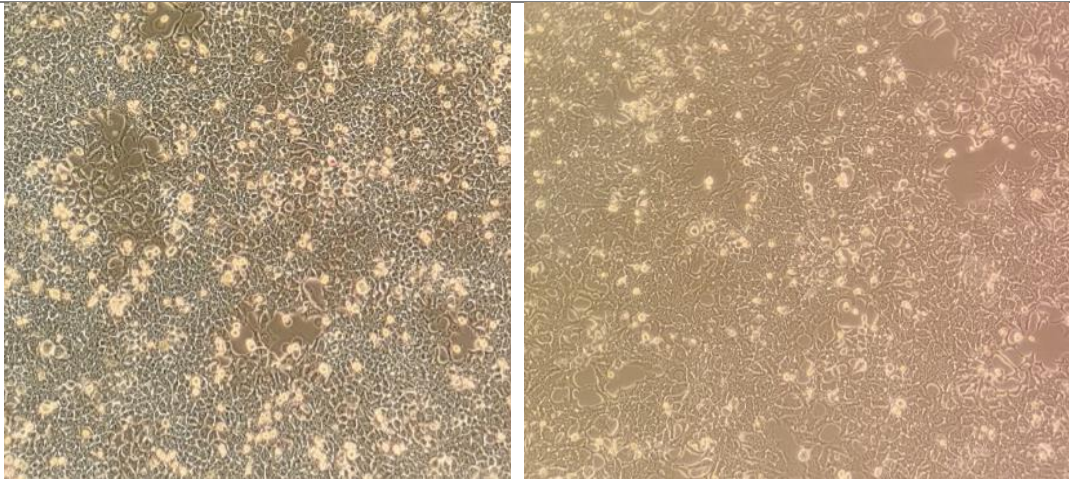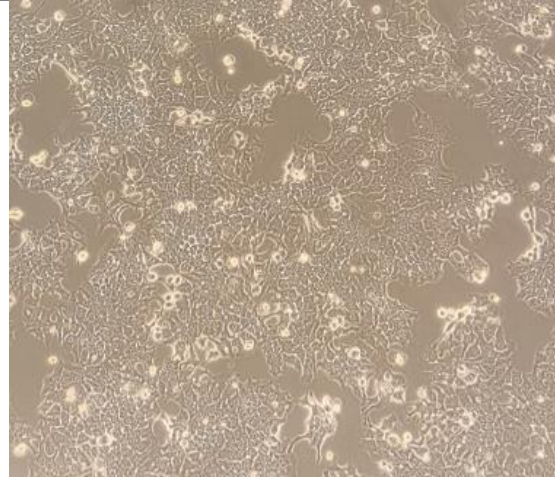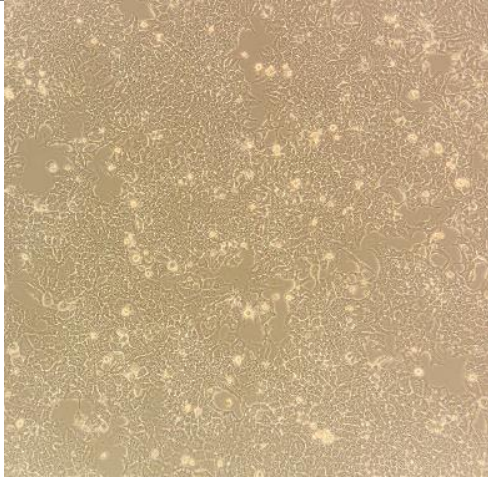
P15-3

P15-4

P15-5

P15-6
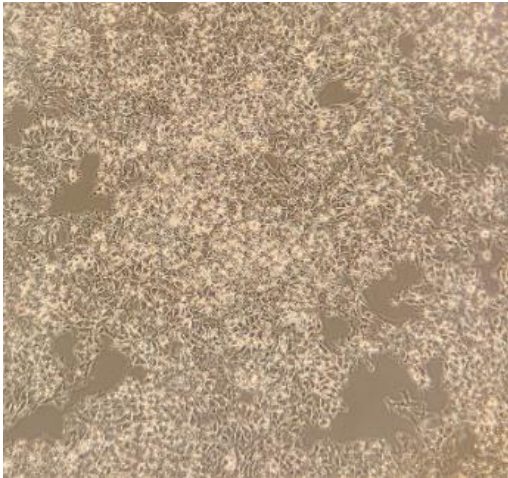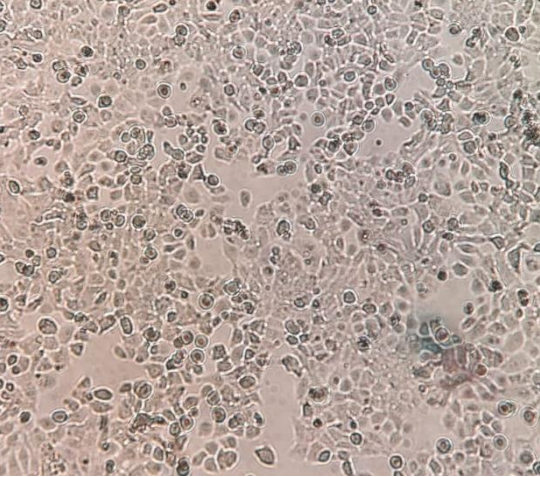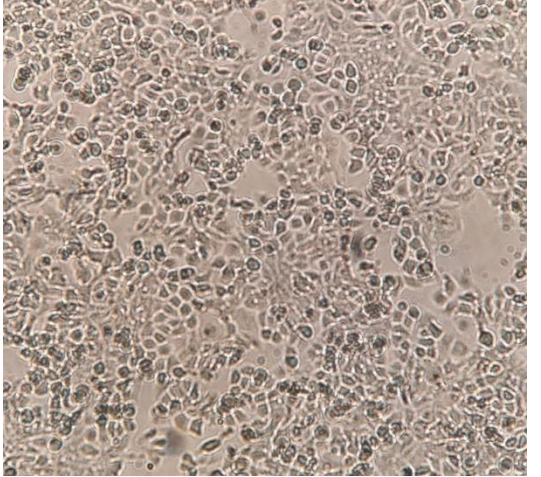
P15-7
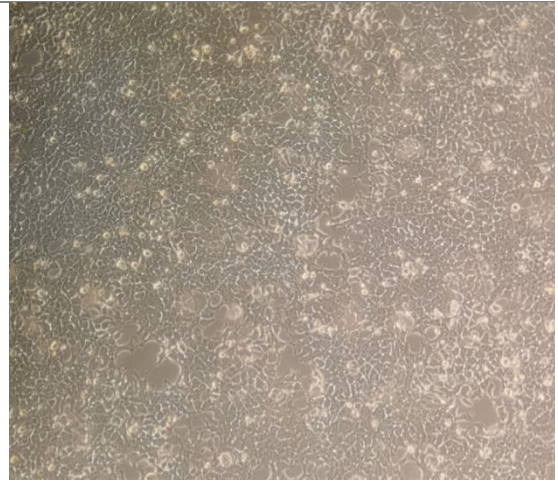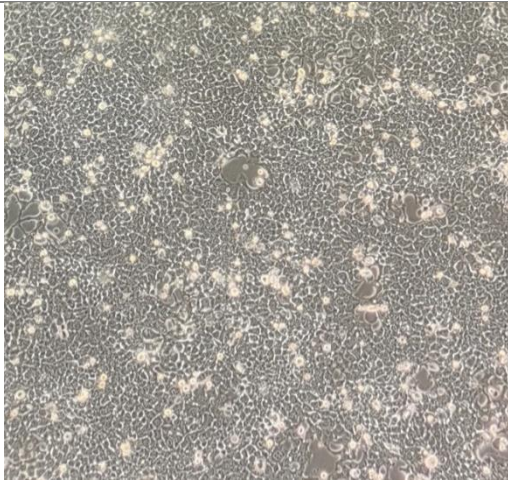
8.2   LTA#2 HuH7 pictures

Appendix Table 2: Pictures from each passage done in the LTA#2 on HuH7. *The 1 µM AFB1 passage died during the LTA#2. Each passage was seeded with 2*10⁶ cells.*

	0,1 µM AFB1	1 µM AFB1
P26-1		
P26-2		

P26-3

P26-4

P26-5

P26-6

P26-7

8.3   Raw data absorbances

Appendix Table 3: Absorbances at 560 nm and 690 nm for HuH7, HepG2 and Mahlavu using the MTT assay and a 24h AFB1 treatment. Raw data for Figure 19.

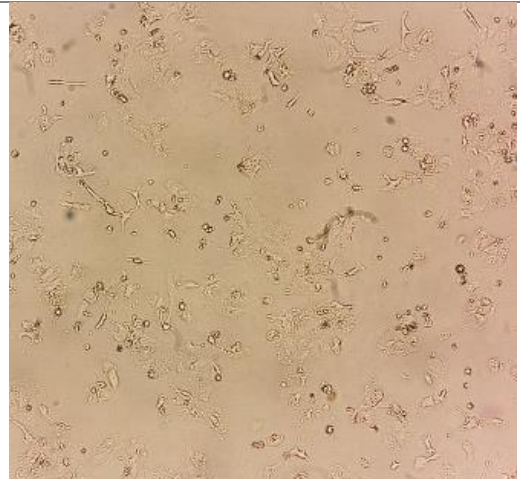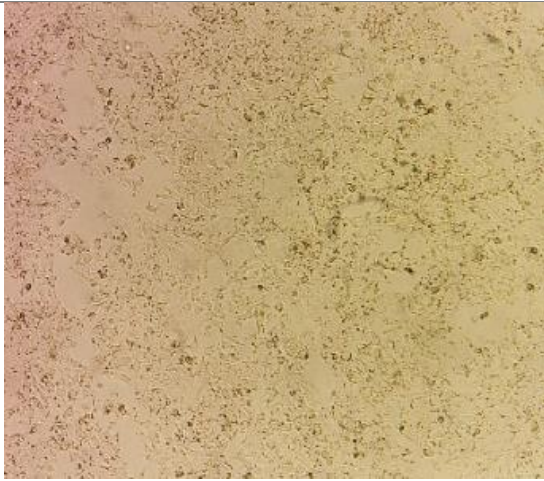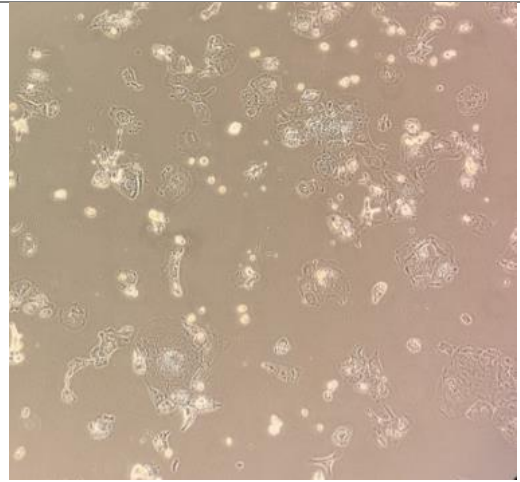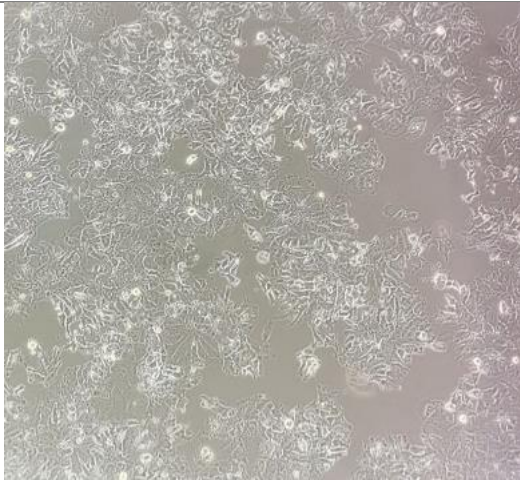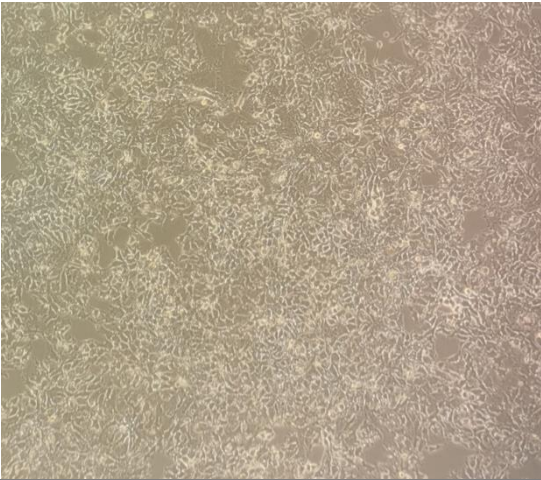| Abs	HuH7				HepG2				Mahlavu			
560 nm												
Only medium	0,1320	0,0527	0,0673	0,1199	0,0863	0,1795	0,1195	0,1768	0,4822	0,0806	0,1130	0,1250
0 µM AfB1	1,1637	0,6635	0,6354	0,6043	1,0068	0,8206	1,0194	0,9331	0,6973	0,6891	0,8170	0,8467
0,01 µM AfB1	0,8090	0,7143	0,6461	0,5912	0,8649	1,1874	1,0741	1,0498	0,7185	0,4445	0,6964	0,7617
0,1 µM AfB1	0,6256	0,5857	0,5858	0,5476	1,0999	1,3372	1,0829	0,7329	0,5564	0,4791	0,6837	0,7818
1 µM AfB1	0,6264	0,5676	0,5142	0,5251	1,1592	1,4047	1,1306	0,7824	0,5087	0,5434	0,6535	0,7154
10 µM AfB1	0,5382	0,5978	0,5393	0,5534	0,8667	1,0361	0,8248	0,8263	0,5973	0,6608	0,6918	0,6328
100 µM AfB1	0,4402	0,3750	0,3530	0,3346	0,4498	0,7510	0,6136	0,5241	0,3163	0,4099	0,4236	0,3867
DMSO	0,4921	0,5587	0,5657	0,5396	0,9732	1,0273	1,4149	1,0915	0,5741	0,3817	0,5243	0,7575
690 nm												
Abs	1	2	3	4	5	6	7	8	9	10	11	12
Only medium	0,1068	0,0464	0,0551	0,0924	0,0680	0,1360	0,0909	0,1408	0,3188	0,0620	0,0833	0,0917
0 µM AfB1	0,3581	0,1007	0,0752	0,0907	0,0824	0,1251	0,1136	0,1429	0,1317	0,0785	0,0838	0,0957
0,01 µM AfB1	0,2322	0,0948	0,0962	0,0901	0,1079	0,1461	0,1190	0,2912	0,1503	0,0844	0,1498	0,0915
0,1 µM AfB1	0,1297	0,0785	0,0677	0,0676	0,0955	0,1297	0,1127	0,0929	0,0953	0,0912	0,0934	0,0992
1 µM AfB1	0,0818	0,0554	0,0512	0,0753	0,1033	0,1210	0,0985	0,0965	0,0829	0,0880	0,0995	0,0875
10 µM AfB1	0,0770	0,0909	0,0574	0,0823	0,0962	0,1168	0,0677	0,1109	0,0713	0,0859	0,1065	0,0710
100 µM AfB1	0,0969	0,0523	0,0506	0,0511	0,0566	0,0790	0,0620	0,0689	0,0671	0,0676	0,0835	0,0633
DMSO	0,0712	0,0611	0,0597	0,0722	0,0735	0,0753	0,1018	0,0834	0,0801	0,0707	0,0702	0,0920

Appendix Table 4: Absorbances at 560 nm and 690 nm for HuH7, HepG2 and Mahlavu using the MTT assay and a 48h AFB1 treatment. Raw data for Figure 19.

Abs	HuH7				HepG2				Mahlavu			
560 nm												
Only medium	0,1736	0,1696	0,1041	0,0984	0,1507	0,0844	0,2813	0,1543	0,0942	0,0699	0,1371	0,0778
0 µM AfB1	0,9360	0,9585	0,9005	0,9501	1,6585	1,3346	1,3947	1,1197	1,3894	1,5754	1,4928	1,4530
0,01 µM AfB1	0,9526	1,0115	0,9935	0,8234	1,5933	1,3149	1,5419	1,3992	1,2523	1,3530	1,6015	1,6346
0,1 µM AfB1	0,9583	0,9154	0,9158	0,8817	1,5794	1,8153	1,6148	1,4729	1,1080	1,1052	1,4781	1,6105
1 µM AfB1	1,0383	0,9052	0,8683	0,8582	1,6341	1,7672	1,6109	1,4507	1,1904	1,2799	1,5493	1,6073
10 µM AfB1	0,7811	0,7498	0,7082	0,6666	1,6530	1,6157	1,6430	1,5092	1,0975	1,1432	1,0896	1,1867
100 µM AfB1	0,2695	0,2572	0,2468	0,2395	1,1514	1,3220	1,2358	0,9244	0,4068	0,5363	0,6547	0,5544
DMSO	0,8204	0,7894	0,9505	0,6525	1,6449	1,8654	1,9233	2,2576	1,0677	1,0854	1,0135	1,3426
690 nm												
Abs	1	2	3	4	5	6	7	8	9	10	11	12
Only medium	0,1353	0,1298	0,0837	0,0785	0,1253	0,0678	0,2347	0,1193	0,0769	0,0587	0,1053	0,0658
0 µM AfB1	0,1095	0,1127	0,1033	0,1378	0,2076	0,1927	0,2041	0,1576	0,1341	0,1605	0,1434	0,1892
0,01 µM AfB1	0,1114	0,1240	0,3647	0,0904	0,1803	0,2152	0,1645	0,1629	0,1293	0,1202	0,1513	0,1617
0,1 µM AfB1	0,1142	0,0937	0,1311	0,1205	0,2029	0,3096	0,1791	0,1511	0,1422	0,1479	0,1886	0,1722
1 µM AfB1	0,1338	0,1003	0,0819	0,1009	0,1885	0,2621	0,1653	0,1862	0,1221	0,1492	0,1586	0,1576
10 µM AfB1	0,0973	0,1000	0,1125	0,0747	0,1586	0,2148	0,1706	0,1714	0,1580	0,1131	0,1118	0,1762
100 µM AfB1	0,0673	0,0805	0,0838	0,0770	0,1427	0,1921	0,1672	0,1644	0,0798	0,1124	0,1071	0,1284
DMSO	0,1401	0,1577	0,3148	0,1079	0,1645	0,2390	0,1972	0,4186	0,1020	0,1580	0,1245	0,1386

Appendix Table 5: Absorbances at 560 nm and 690 nm for HuH7, HepG2 and Mahlavu using the MTT assay and a 72h AFB1 treatment. Raw data for Figure 19.

Abs	HuH7				HepG2				Mahlavu			
560 nm												
Only medium	0,1030	0,1734	0,1782	0,1261	0,0832	0,1119	0,1056	0,1260	0,1254	0,1941	0,4552	0,1107
0 µM AfB1	1,2271	1,3044	1,2505	1,1311	1,6676	1,6732	1,3926	1,5755	1,7748	1,5134	1,5588	1,8415
0,01 µM AfB1	1,4478	1,2790	1,1240	1,1289	1,5964	1,5450	1,3840	1,5078	1,4216	1,4142	1,6161	1,5808
0,1 µM AfB1	1,1289	1,1794	1,2074	1,0961	1,5364	1,5252	1,5029	1,3753	1,3901	1,4345	1,5949	1,5843
1 µM AfB1	1,3453	1,2093	1,0865	0,5800	1,6580	2,0184	1,3923	1,4650	1,7924	1,5641	1,5680	1,2709
10 µM AfB1	0,8125	0,7884	0,8628	0,7049	1,8108	1,6126	1,4278	1,3488	1,9576	1,2625	1,3178	1,3109
100 µM AfB1	0,1520	0,1463	0,2036	0,1510	1,0719	1,0264	1,2953	0,8884	0,4765	0,4530	0,5138	0,6423
DMSO	0,9375	1,0341	1,1161	1,0332	1,7436	1,6415	1,6222	1,3615	1,3197	1,5213	1,4685	1,7444
690 nm												
Abs	1	2	3	4	5	6	7	8	9	10	11	12
Only medium	0,0821	0,1454	0,1483	0,1005	0,0665	0,0889	0,0855	0,1002	0,1013	0,1696	0,3523	0,0891
0 µM AfB1	0,2160	0,1666	0,1835	0,1470	0,2616	0,2513	0,2299	0,2036	0,3907	0,1198	0,1761	0,1380
0,01 µM AfB1	0,8130	0,1810	0,1510	0,1316	0,2138	0,2378	0,2307	0,1836	0,1526	0,1398	0,1835	0,1391
0,1 µM AfB1	0,1117	0,1467	0,1853	0,1580	0,1948	0,2156	0,2134	0,1815	0,1252	0,1763	0,1749	0,1323
1 µM AfB1	0,1879	0,2138	0,1580	0,3345	0,2274	0,5658	0,2250	0,1613	0,4373	0,1576	0,1835	0,1236
10 µM AfB1	0,1260	0,0976	0,2094	0,1261	0,2979	0,1731	0,1607	0,1490	0,6724	0,1650	0,1672	0,1454
100 µM AfB1	0,0948	0,0793	0,1282	0,0857	0,1380	0,1512	0,2286	0,1697	0,1104	0,0910	0,1116	0,1780
DMSO	0,1278	0,1440	0,1915	0,1693	0,2042	0,1759	0,2085	0,1466	0,2262	0,1783	0,1285	0,6200